Fraction of the Dark Current Carried by Ca^{2+} through cGMP-gated Ion Channels of Intact Rod and Cone Photoreceptors

Tsuyoshi Ohyama,* David H. Hackos,* Stephan Frings,‡ Volker Hagen,§
U. Benjamin Kaupp,‡ and Juan I. Korenbrot*

From the *Department of Physiology and Graduate Program in Biophysics, School of Medicine, University of California at San Francisco, San Francisco, California 94143; ‡Institut für Biologische Informationsverarbeitung, Forschungszentrum Jülich, 52425 Jülich, Germany; and §Forschungs institut für Molekulare Pharmakologie, 10315 Berlin, Germany

ABSTRACT The selectivity for Ca^{2+} over Na^+, PCa/PNa, is higher in cGMP-gated (CNG) ion channels of retinal cone photoreceptors than in those of rods. To ascertain the physiological significance of this fact, we determined the fraction of the cyclic nucleotide–gated current specifically carried by Ca^{2+} in intact rods and cones. We activated CNG channels by suddenly (<5 ms) increasing free 8Br-cGMP in the cytoplasm of rods or cones loaded with a caged ester of the cyclic nucleotide. Simultaneous with the uncaging flash, we measured the cyclic nucleotide–dependent changes in membrane current and fluorescence of the Ca^{2+}-binding dye, Fura-2, also loaded into the cells. The ratio of changes in fura-2 fluorescence and the integral of the membrane current, under a restricted set of experimental conditions, is a direct measure of the fractional Ca^{2+} flux. Under normal physiological salt concentrations, the fractional Ca^{2+} flux is higher in CNG channels of cones than in those of rods, but it differs little among cones (or rods) of different species. Under normal physiological conditions and for membrane currents ≤200 pA, the Ca^{2+} fractional flux in single cones of striped bass was 33 ± 2%, and 34 ± 6% in catfish cones. Under comparable conditions, the Ca^{2+} fractional flux in rod outer segments of tiger salamander was 21 ± 1%, and 14 ± 1% in catfish rods. Fractional Ca^{2+} flux increases as extracellular Ca^{2+} rises, with a dependence well described by the Michaelis-Menten equation. *K*Ca, the concentration at which Ca^{2+} fractional flux is 50% was 1.98 mM in bass cones and 4.96 mM in tiger salamander rods. Because Ca^{2+} fractional flux is higher in cones than in rods, light flashes that generate equal photocurrents will cause a larger change in cytoplasmic Ca^{2+} in cones than in rods.

KEY WORDS: retina • phototransduction • ion selectivity

INTRODUCTION

In rod and cone photoreceptors of the vertebrate retina, a continuous membrane current flows into the outer segment in the dark that light suppresses. The dark current is carried by the simultaneous inward flux of Na^+, Ca^{2+}, and Mg^{2+} ions (Hodgkin et al., 1985; Cervetto et al., 1988) flowing through cyclic nucleotide–gated (CNG)[1] ion channels. Understanding the fraction the dark current specifically carried by Ca^{2+} ions is important because Ca^{2+} influx, as a component of the dark current, is in a dynamic balance with its efflux through a $Na^+/Ca^{2+},K^+$ exchanger, and this balance determines the free cytoplasmic Ca^{2+} in the outer segment of rods and cones (Yau and Nakatani, 1985; Miller and Korenbrot, 1987; Lagnado et al., 1992). Moreover, the quantitative features of both influx and efflux differ between rods and cones, and these differences contribute to explaining the difference in transduction signals between the two photoreceptor types (Korenbrot, 1995).

The fraction of the dark current carried by any given ion depends on the ion selectivity of the CNG channels and the concentration and driving force of that ion. CNG channels in rods and cones are more permeable to Ca^{2+} than to Na^+, but they differ in their relative selectivity of Ca^{2+} over Na^+ (PCa/PNa). Under saturating concentrations of cGMP, when the probability of channel opening is ~0.9, and in the presence of simple bionic solutions, PCa/PNa in cones is ~21.7, but in rods it is ~6.5 (Picones and Korenbrot, 1995; Wells and Tanaka, 1997; Hackos and Korenbrot, 1999). The difference in PCa/PNa between CNG channels of rods and cones is also observed in recombinant channels formed from alpha subunits alone (Frings et al., 1995). The value of PCa/PNa changes with channel gating: at the cGMP concentrations expected in intact cells, when probability of channel opening is ~0.03, PCa/PNa in cones is ~7.4× larger than that in rods (Hackos and Korenbrot, 1999).

To understand the functional significance of the differences in ion selectivity between rod and cone CNG channels, the fraction of the dark current carried by

Dr. Hackos' present address is Molecular Physiology and Biophysics Unit, National Institute of Neurological Disease and Stroke, National Institutes of Health, Bethesda, MD 20892.116

Address correspondence to Juan I. Korenbrot, Dept. of Physiology, School of Medicine, Box 0444, University of California at San Francisco, San Francisco, CA 94143. Fax: 415-476-4929; E-mail: juan@itsa.ucsf.edu

[1]*Abbreviations used in this paper:* bu, bead unit; CNG, cyclic nucleotide–gated; dROS, detached rod outer segment; IBMX, 3-isobutyl-1-methylxanthine; PDE, phosphodiesterase; PMT, photomultiplier tube.

Ca^{2+} under physiological solutions needs to be computed from the known values of PCa/PNa. This task, however, is complex. It may be accomplished through theoretical models of ion permeation. For example, Wells and Tanaka (1997) elegantly developed an Eyring-type permeation model for CNG channels with three barriers, two wells, and four sites (each for Na^+, K^+ Ca^{2+}, and Mg^{2+}) that simulates fractional currents and permeability ratios. A comparably complete computation has not been reported for cone CNG channels.

The fraction of the dark current carried by Ca^{2+} in intact rod has been experimentally estimated using an indirect method. The method depends on measurements of a membrane current generated by the electrogenic transport of cations by the $Na^+/Ca^{2+},K^+$ exchanger, and requires the separation of this electrogenic current from a changing conductive current. The method has limitations that have been thoroughly considered by those who have used it (Nakatani and Yau, 1988). Despite its possible limitations, the method in several hands has provided a reproducible estimate that in rods, between 10 and 20% of the dark current is carried by Ca^{2+} (Nakatani and Yau, 1988; Lagnado et al., 1992; Gray-Keller and Detwiler, 1994; Younger et al., 1996). The $Na^+/Ca^{2+},K^+$ exchanger in cones also generates an electrogenic current. This current, however, is at least an order of magnitude faster than that measured in rods (Nakatani and Yau, 1989; Hestrin and Korenbrot, 1990; Perry and McNaughton, 1991). Separating the electrogenic from the photocurrent, hence, is fraught with error (our unpublished observation) and analysis of the Ca^{2+} fractional current in cones through this method is not entirely reliable.

Recently, Neher and his collaborators developed a method to assess the fraction of current carried specifically by Ca^{2+} in several voltage- and ligand-gated channels (reviewed in Neher, 1995). The method depends on the simultaneous measurement of membrane current and cytoplasmic Ca^{2+} after synchronous activation of the channels of interest. We have previously extended this method to an investigation of the fractional Ca^{2+} flux in recombinant CNG channels formed by alpha subunits of olfactory, rod, and cone receptor cells (Dzeja et al., 1999; Frings et al., 2000). We report here on the application of this method to studies in rod and cone photoreceptors that have allowed us to directly determine the fraction of the dark current carried by Ca^{2+} in intact cells isolated from several species.

MATERIAL AND METHODS

Materials

Striped bass (*Morone saxitilis*) and catfish (*Ictalurus punctatus*) were obtained from Professional Aquaculture Services and maintained in the laboratory for up to 6 wk under 10:14-h dark:light cycles. Tiger salamanders (*Ambystoma tigrinum*) were received from Charles Sullivan and maintained in an aquarium at 6°C under 12:12-h dark:light cycles. Gecko (*Gecko gecko*) were obtained from local shops and maintained at ambient temperature under normal daylight cycles. The UCSF Committee on Animal Research approved protocols for the upkeep and killing of the animals.

Caged 8-Br-cGMP (8-bromoguanosine 3′, 5′-cyclic monophosphate, 4,5-dimethoxy-2-nitrobenzyl ester, dihydrate, axial isomer) was synthesized as previously described (Hagen et al., 1996, 1998). Fura-2 was purchased from TefLabs. Enzymes for tissue dissociation were obtained from Worthington Biochemical. All other chemicals were from Sigma-Aldrich.

Photoreceptor Isolation

Under infrared illumination and with the aid of a TV camera and monitor, retinas were isolated from dark-adapted animals and photoreceptors were dissociated as described in detail elsewhere (Miller and Korenbrot, 1993, 1994). Single cones were isolated by mechanical trituration of fish retinas briefly treated with collagenase and hyaluronidase. Chopping the retina with a blade isolated rod outer segments. Photoreceptors were isolated and maintained in a Ringer's solution specific to each species studied. Solution composition is listed in Table I.

Photoreceptors were dissociated in a Ringer's solution in which glucose was replaced with 5 mM pyruvate. Suspended in this solution, cells were added to a recording chamber held on the stage of an inverted microscope. The bottom of the recording chamber was a glass coverslip derivatized with Concanavalin A (Picones and Korenbrot, 1992). Solitary photoreceptors were firmly attached to the coverslip, and after 5 min the bath solution was exchanged with the normal, glucose-containing Ringer's.

Electrical Recording and Solutions

Photoreceptors in the recording chamber were observed using an inverted microscope equipped with differential interference contrast optics and operated under infrared light (850 ± 40 nm) with the aid of an IR-sensitive TV camera and monitor. We measured membrane currents under voltage clamp at room temperature using tight-seal electrodes in the whole-cell mode. Electrodes were produced from aluminosilicate glass (1.5 mm o.d. × 1.0 mm i.d., No. 1724; Corning Glassworks), and were sealed onto the side of detached rod outer segments or the inner segment of isolated single cones. Currents were measured with a patch-clamp amplifier (Axopatch 1D; Axon Instruments, Inc.). Analogue signals were low-pass filtered below 200 Hz with an eight-pole Bessel filter (Kronh-Hite), and then digitized on line at 1 kHz (FastLab; Indec).

Solutions used to fill tight-seal electrodes are listed in Table II. Salt solutions were first passed over a Chelex-100 resin column (Bio-Rad Laboratories) to thoroughly remove all multivalent cations; $MgCl_2$ was then added. Fura-2 and caged 8Br-cGMP were added to the solutions immediately before use. Even in the dark, caged 8Br-cGMP hydrolyzes over time (Hagen et al., 1998). Therefore, electrode-filling solutions were kept in darkness and discarded after 3 h.

Solutions used to measure cGMP-gated currents with Ca^{2+} as the exclusive net charge carrier are listed in Table III. In these solutions, the permeant cations Na^+ and Mg^{2+} were replaced by the impermeant cations $choline^+$ or $tetramethylamonium^+$ (Hodgkin et al., 1985). K^+ was not replaced because its presence is required for the function of the $Na^+/Ca^{2+},K^+$ exchanger. However, its concentrations were selected such that at −35 mV the holding voltage in the experiments, the net K^+ current was zero.

TABLE I

Composition of Extracellular Ringers Solutions Used to Isolate and Perfuse Solitary Photoreceptors

	Striped bass	Catfish	Gecko	Tiger salamander
NaCl*	143	125	143	100
KCl	2.5	2.5	2.5	2
$NaHCO_3$	5	5	5	5
NaH_2PO_4	1	5	1	1
$CaCl_2$	1	1	1	1
$MgCl_2$	1	1	1	1
glucose	10	10	10	10
HEPES	10	10	10	10
pH	7.5	7.4	7.5	7.4
Osmotic pressure‡	310	280	310	227

Salts are given in millimolar. *In addition to the salts listed, all solutions contained 1× minimum essential medium vitamins and aminoacids. ‡Osmotic pressure is given in milliosmoles.

TABLE II

Composition of Solutions Used to Fill Tight-seal Electrodes

	Striped bass	Catfish	Gecko	Tiger salamander
K gluconate	115	92.5	115	69
K aspartate	20	20	20	20
KCl	33	30	33	30
$MgCl_2$	0.5	0.5	0.5	0.5
Fura-2	2	2	2	2
Caged 8Br-cGMP	0.05	0.05	0.05	0.05
MOPS	10	10	10	15
pH	7.25	7.25	7.25	7.25
Osmotic pressure*	305	272	305	226

Salts are given in millimolar. *Osmotic pressure is given in milliosmoles.

Single-Cell Loading and Superfusion

Photoreceptors in the recording chamber were maintained in darkness under Ringer's solution that was exchanged intermittently. For each cell type studied here, we determined the interval necessary for equilibration between electrode lumen and cytoplasmic spaces by (a) photometrically monitoring the rate of fura-2 loading, and (b) electrically monitoring the rate of change in holding current.

The extracellular solution was changed only around the cell under investigation, using a micro-superfusion system. Test solutions were selected with electronically controlled switch valves and steady flow was maintained under a positive pressure of ~10 cm H_2O. Solutions were delivered through a glass capillary 100 μm in tip diameter placed within ~300 μm of the cell.

Photometric Recording

Simultaneously with membrane current, we measured the fluorescence of single fura 2–loaded photoreceptors. The instrument designed for these studies is schematically illustrated in Fig. 1. Fluorescence excitation light at 380 nm (selected with a narrow band interference filter from a DC powered Xenon source (150W; Osram XBO) was delivered onto the cell through the microscope objective used to observe it (Fluor 40, 40×, 1.3 NA; Nikon). To this end, we designed an epi-illumination pathway consisting of a fiber-optic light scrambler that provided extremely uniform illumination to the back aperture of the objective (Technical Video Ltd.) and a custom dichroic mirror that reflected >60% of light between 300 and 400 nm and transmitted >90% of light between 750 and 950 nm (Chroma Technology). This pathway also included a shutter and an adjustable aperture to selectively deliver fluorescence excitation light to a limited section of the solitary photoreceptors.

We designed a second epi-illumination pathway to deliver to the cell brief, powerful flashes of light to uncage 8Br-cGMP. This pathway consisted of a Xenon flashlamp, able to deliver 200 J with ~170-μs half bandwidth (Chadwick-Helmuth Co.). Uncaging flashes were of light <400 nm, selected with the use of short-pass optical filters (Hoya Optics Inc.). Uncaging light was focused onto the cell through the microscope objective with the aid of a custom designed relay lens. With the use of an adjustable aperture placed in this pathway, the uncaging light could illuminate selected parts of the cell. In general, uniform uncaging flashes were delivered over the entire surface of detached rod outer segments, but were restricted to the outer segment alone in studies of cones.

The fluorescent light emitted by a solitary photoreceptor was captured with a custom micro-objective designed to efficiently capture photons, while allowing electrical recording with microelectrodes (Optical Design Service). The micro-objective is a water immersion, multi-element lens 5.2 mm in diameter, 0.6 NA, and 2.8-mm working distance mounted on a micromanipulator. The lens produces a well-corrected image at a focal length of 10 mm with 0.18 NA. At the focal plane of the micro-objective, we placed the end of a multimode optical fiber (365 μm core, 400 μm clad, step index 0.22 NA). The other end of the fiber was focused, through a coupling lens, onto the photocathode of a photomultiplier tube (PMT) (R943-02; Hamamatsu) operated at −20°C and sampled in 50-ms counting bins using photon-counting instrumentation (Photochemical Research Associates).

The fiber-optic bench incorporated an interference filter to select the emitted fluorescence in the range between 410 and 600 nm (Omega Optical). A synchronized shutter in the bench was used to insure that light from the uncaging Xe flash did not reach the PMT. The fiber-optic bench also included a dichroic mirror and lens to focus the light from an IR laser diode (830 nm) onto the back end of the transfer optical fiber (Oz Optics, Ltd.). This feature was essential because it allowed us to locate and focus the micro-objective onto the individual cell under investigation. The light from the IR laser diode, transferred through the optical fiber, was emitted by the micro-objective. The experimenter, observing through the microscope objective, could see this IR light and use it as a guide to accurately position and focus the micro-objective.

Calibration

In every experiment, a calibrated photodiode (United Detector Technology) was used to measure the intensity of the 380-nm fluorescence excitation light at the position of the cells on the microscope stage. Data presented here were measured at excitation intensities between 1.1 and 1.8×10^8 photons $\mu m^{-2} s^{-1}$. To quantitate cell fluorescence intensity, at the end of each experiment, we measured the fluorescence emitted by individual fluorescent beads excited identically to the cells (Fluoresbrite™ carboxy BB 4.1 ± 0.2 μm microspheres; Polyscience, Inc.). Fluorescence intensity of cells and beads was corrected by subtracting from each the signal measured in their absence and due to leakage of light between excitation and emission filter sets (cross talk). In each experiment, we averaged the fluorescence of 10 different beads (units of counts in 50-ms bin per bead) and defined this intensity

TABLE III

Composition of Solutions Used to Measure f_{max}

	Stripped bass		Catfish		Gecko		Tiger salamander	
	Extracellular	Intracellular	Extracellular	Intracellular	Extracellular	Intracellular	Extracellular	Intracellular
CholineCl	152						120	
Choline gluconate		145	126	120				108
Choline aspartate			10	10				
TMACl*					152	145		
KCl	2.5	10	2.5	10	2.5	10	2.5	10
$CaCl_2$	1		1		1		1	
Fura-2		2		2		2		2
Caged 8Br-cGMP		0.05		0.05		0.05		0.05
MOPS	10	10	10	10	10	10	7.5	7.5
pH‡	7.5	7.25	7.5	7.25	7.5	7.25	7.4	7.25
Osmotic pressure§	306	305	279	279	306	305	226	224

Salts are given in millimolar. *Tetramethylammonium; ‡titrated with either TMAOH or NMDG, both impermeant cations; §osmotic pressure is given in milliosmoles.

as one bead unit (bu). Cell fluorescence was expressed in bu by dividing the intensity of each cell by the bead unit measured in the same experiment.

Data Analysis

To calculate P_f, the fractional Ca^{2+} flux, we corrected the data to analyze only the flash-dependent changes. To this end, we averaged the value of the holding current and fluorescence for 1 s preceding the uncaging flash and subtracted this value from the data; consequently, both the holding current and the fluorescence intensity preceding the flash had an average value of zero. We then integrated the corrected current over the first 15 s after the uncaging flash. Finally, we fit the integral of the current changes to the fluorescence changes.

Selected mathematical functions were fit to experimental data with nonlinear, least square minimization algorithms (Origin; MicroCal Software). Dynamic simulations were carried out using Tutsim™ software (Actuality Corp.). Statistical error throughout is presented as SD. In some calculations of population mean, we included two, and only two, measurements from the same cell (as indicated in the text). To calculate errors on ratios of means, we

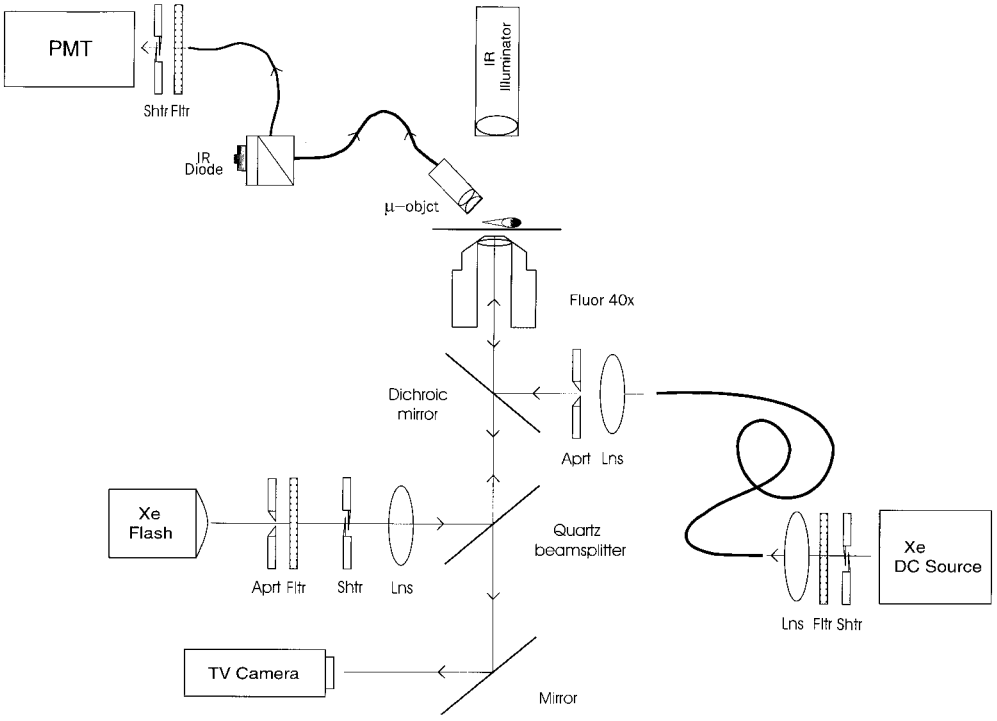

FIGURE 1. Schematic illustration of microfluorimeter designed to simultaneously measure membrane current and fluorescence from individual, solitary rod, and cone photoreceptors. The photoreceptors are observed under infrared differential interference contrast with the aid of a TV camera. Fluorescence excitation light from a Xe source is selected at 380 nm with interference filters and delivered onto the cell through an epi-illumination path consisting of a fiber-optic scrambler, a dichroic mirror, and a lens that permits an adjustable aperture to be focused onto selected areas of the cell. Uncaging light from a Xe flash source is selected below 400 nm with short pass filters and delivered onto the cell through an epi-illumination path consisting of a quartz beam splitter and a relay lens that permits an adjustable aperture to be focused onto selected areas of the cell. Fluorescence emission in the range between 400 and 600 nm is collected by a custom micro-objective (μ-objct) that focuses the image of the cell onto the end of an optical fiber. This fiber is part of a fiber optic bench that delivers the collected photons to a PMT operated in photon counting mode.

computed propagation of errors as described by Bevington (1992):

$$a = \pm\frac{u}{v}$$

$$\frac{\sigma_a^2}{a^2} = \frac{\sigma_u^2}{u^2} + \frac{\sigma_v^2}{v^2},$$

where σ^2 is the variance of the mean of quantities a, u and v.

Theory

The fraction of the cGMP-dependent current carried by Ca^{2+} ions in photoreceptors, here denominated P_f, can be determined by simultaneously measuring total membrane current with patch-clamp electrodes, and Ca^{2+} concentration with the Ca^{2+}-sensitive fluorescent dye, fura-2. Neher (1995) has reviewed this analytical method and we have described in detail its application to studies of CNG channels (Frings et al., 2000). In brief, cGMP-dependent currents are rapidly activated by the sudden intracellular application of 8Br-cGMP, achieved by photolysis of caged 8Br-cGMP molecules. Because the channels exhibit only limited ion selectivity, the cGMP-dependent membrane current in normal Ringer's solution, I_T, is composed of contributions from several ion species: Na^+ (I_{Na}), K^+ (I_K), Mg^{2+} (I_{Mg}), and Ca^{2+} (I_{Ca}) (Eq. 1):

$$I_T = I_{Na} + I_K + I_{Ca} + I_{Mg}. \quad (1)$$

The Ca^{2+}-free form of fura-2 is present in the outer segment's cytoplasm, where it binds the inflowing Ca^{2+}. Binding Ca^{2+} causes a decrease in the intensity of fluorescence excited by 380 nm light (F380). The extent of decline in F380 is proportional to free Ca^{2+} concentration, but it measures the total amount of Ca^{2+} entering the cell if, and only if, a number of experimental conditions are strictly met. (a) Ca^{2+} enters the cell only through the channels of interest. (b) All entering Ca^{2+} is bound by free fura-2; none is sequestered or actively transported out of the cell. (c) Fura-2 outcompetes endogenous Ca^{2+} buffers because it is present at a concentration that exceeds that of the other buffers. The change in the mole amount of intracellular Ca^{2+} caused by the cGMP-activated current over a time interval Δt, is given by Eq. 2:

$$\Delta n_{in} = \frac{1}{2F}\int_0^{\Delta t} I_{Ca}(t)\,dt, \quad (2)$$

where F is Faraday's constant. If fura-2 is used to monitor cytoplasmic Ca^{2+}, intracellular Ca^{2+} may distribute among several competing pools: (a) free Ca^{2+}, (b) Ca^{2+} bound to cytoplasmic buffers (CaB), (c) Ca^{2+} bound to fura-2 (CaFu), and (d) Ca^{2+} pumped into cellular organelles or out of the cell (P). Thus:

$$\Delta n_{in} = \Delta n_{free} + \Delta n_{CaFu} + \Delta n_{CaB} + \Delta n_P, \quad (3)$$

where Δn_{free}, Δn_{CaFu}, Δn_{CaB}, and Δn_P are the changes in mole amount of Ca^{2+} free, bound to fura-2, bound to cytoplasmic buffers, and pumped (or sequestered) out of the cytoplasm, respectively. Neher (1995) reasoned, and proved rigorously, that under certain experimental conditions, when all entering Ca^{2+} is bound to the fura-2 present in the cell, Eq. 3 can be simplified. These conditions are: (a) measurements are executed with high fura-2 concentrations, 1–5 mM. Under this condition, the indicator dye, which is a very powerful buffer, outcompetes the endogenous Ca^{2+} buffers, rendering Δn_{CaB} negligible. (b) The rapid rate of Ca^{2+} binding by fura-2 (few milliseconds) (Kao and Tsien, 1988) allows a few seconds to be sufficiently long for binding to the dye to be complete, but still short relative to the time necessary to pump Ca^{2+} into organelles or out of the cell; this condition makes Δn_P negligible. (c) Fura-2 exists in its Ca^{2+}-free form. Then, all entering Ca^{2+} is bound by the dye and Δn_{free} is negligible. Then, only under these experimental conditions:

$$\Delta n_{in} = \Delta n_{CaF} = \frac{1}{2F}\int_0^{\Delta t} I_{Ca}(t)\,dt, \quad (4)$$

The Ca^{2+} binding capacity of fura-2, κ_{Fu} is defined as (Eq. 5):

$$\kappa_{Fu} = \frac{d[CaFu]}{d[Ca^{2+}]} = \frac{K_d[Fu]_{tot}}{(K_d + [Ca^{2+}])^2}, \quad (5)$$

where $[Ca^{2+}]$, [CaFu], and $[Fu_{tot}]$ are the concentrations of free Ca^{2+}, bound Ca^{2+}, and total fura-2, respectively. K_d is the dissociation constant of the fura-Ca^{2+} complex. With this definition, considering a small incremental elevation in $[Ca^{2+}]$ and under the experimental conditions that hold true for Eq. 4, then:

$$\Delta n_{in} = V_c\Delta[Ca^{2+}](1 + \kappa_{Fu}), \quad (6)$$

where V_c is the accessible cytoplasmic volume. If we define the emitted intensity of fura-2 fluorescence excited at 380 nm (F_{380}) as the sum of the fluorescence of its two molecular forms, one Ca^{2+}-free, S_{Fu}, and the other Ca^{2+}-bound, S_{CaFu}, then:

$$\Delta F_{380} = \frac{\Delta n_{in}(S_{CaFu} - S_{Fu})\kappa_{Fu}}{1 + \kappa_{Fu}} = V_c\Delta[Ca^{2+}](S_{CaFu} - S_{Fu})\kappa_{Fu}. \quad (7)$$

This equation indicates that, under these conditions, the change in fluorescence is proportional to the total amount of Ca^{2+} entering the cell, as the ion shifts the fraction of fura-2 between its free and bound states. Combining Eqs. 4, 6, and 7 yields Eq. 8:

$$\frac{\Delta F_{380}}{\int_0^{\Delta t} I_{Ca}(t)\,dt} = (S_{CaFu} - S_F)\frac{\kappa_{Fu}}{1 + \kappa_{Fu}}. \quad (8)$$

Let us define f as the ratio of the change in fluorescence, ΔF_{380}, and the integral of the membrane current (Eq. 9):

$$f = \frac{\Delta F_{380}}{\int_0^{\Delta t} I_T(t)\,dt}. \quad (9)$$

Under conditions where Ca^{2+} is the exclusive current carrier; that is, when $I_T = I_{Ca}$, then f takes the value f_{max}.

$$f_{max} = \frac{\Delta F_{380}}{\int_0^{\Delta t} I_{Ca}(t)\,dt}, \quad (10)$$

and the fraction of the I_T current carried by Ca^{2+} under normal conditions, P_f, can be calculated if f and f_{max} are both measured in the same cell type.

$$P_f = \frac{f}{f_{max}}. \quad (11)$$

RESULTS

To determine P_f, the fraction of the total cGMP-dependent current carried by Ca^{2+} ions, we measured flash-generated changes in membrane current under voltage clamp and fluorescence of individual rod and cone photoreceptors loaded with caged 8Br-cGMP and fura-2. We studied the cells with tight-seal electrodes filled with solutions that lacked triphosphate nucleotides and, therefore, could not sustain endogenous synthesis of cGMP (Hestrin and Korenbrot, 1987; Rispoli et al., 1993). At −35 mV holding voltage, the magnitude of the membrane current preceding the uncaging flash is a measure of the stability of the electrical recordings and the completeness of diffusion exchange between electrode lumen and the cytoplasm. When the cells' cytoplasm is fully equilibrated with the electrode lumen, the holding current, Ihold, at −35 mV should be zero for detached rod outer segments (dROS) and outward for cones, which consist of both inner and outer segments. These expectations follow from the fact that CNG channels are the only channels in the dROS and they should be closed (Baylor and Nunn, 1986). In cones, and rods with an inner segment, in contrast, an outward current can be expected to flow through the voltage-dependent K^+ channels of the inner segment (Maricq and Korenbrot, 1990; Barnes and Hille, 1989). The data presented here were measured in tiger salamander dROS no less than 4.5 min after going into whole-cell mode and while Ihold was −4.6 ± 2.7 pA (n = 17); striped bass single cones at no less than 3 min after going into whole-cell mode and while Ihold was 21.1 ± 12.3 pA (n = 35); catfish cones at no less than 3 min after going into whole-cell mode and while Ihold was 14.3 ± 8.3 pA (n = 11), and catfish rods (which retain a portion of their inner segment) at no less than 4 min after going into whole-cell mode and while Ihold was 46.2 ± 16.7 pA (n = 12). Cell fluorescence of fura-2 also confirmed that, at the times indicated, equilibration between cell cytoplasm and the electrode was complete.

Typical current and fluorescence changes generated by uncaging flashes in dROS of tiger salamander and single cones of striped bass are illustrated in Fig. 2. In both receptor types, the uncaging flash activated a transient, inward current and, simultaneously, caused a decrease in fluorescence intensity. The current increase reflects the transient opening of cGMP-gated channels, while the loss of fluorescence arises from the entry of Ca^{2+} ions, which subsequently bind to fura-2. Shown are repeated measurements in the same cell generated by flashes of increasing intensity. Photoreceptors recovered to their initial conditions in between flashes, provided that at least 3 min elapsed between the flashes. The peak current amplitude increased with flash intensity and so did the extent of fluorescence change. Since the intensity of the flash is correlated with the amount of released 8Br-cGMP, the results indicate that current amplitude and Ca^{2+} influx are dependent on the cyclic nucleotide concentration. Since CNG channels in rods are more sensitive to 8Br-cGMP than those of cones (Hackos and Korenbrot, 1997), it is not surprising that uncaging flashes of comparable intensity caused larger current changes in rods than in cones.

The rapid rise of the flash-generated current (time to peak ≤100 ms) (Fig. 2) is consistent with the rate of photolysis of the caged 8Br-cGMP (Hagen et al., 1998) and the rapid activation of channels by the free nucleotide (Karpen et al., 1988). However, the rapid decline from a peak towards the starting value is surprising. We observed this feature in every cell and every species we studied. The time course of the current decay from its peak was well described by a single exponential. In tiger salamander dROS, the mean decay time constant was 0.84 ± 0.23 s (range 0.61–1.27, n = 13 for peak currents ≤200 pA). In striped bass cones, the mean decay time constant was 0.89 ± 0.38 s (range 0.54–1.77 s, n = 9 for peak currents ≤200 pA). Experimental results detailed in the APPENDIX suggest that the rapid current decline arises primarily from the binding of free 8Br-cGMP to specific binding sites in the outer segment. The existence of cGMP-binding sites in rod outer segments has been inferred from analysis of cGMP diffusion kinetics (Olson and Pugh, 1993; Koutalos et al., 1995) and measured biochemically (Cote and Brunnock, 1993). Although comparable data do not exist for cones, the similarity in decay kinetics suggests that cGMP-binding sites are not different in rods and cones.

Experimental Conditions Required to Determine the Value of P_f Are Met in Isolated Photoreceptors

To calculate P_f, it is crucial to establish that the experimental conditions necessary to apply the analytical theory described above indeed hold.

Ca^{2+} enters the cell only through the channels of interest. In dROS, CNG are the only ion channels present in the plasma membrane (Baylor and Nunn, 1986; Hestrin and Korenbrot, 1987). In cones, and rods with an inner segment, Ca^{2+} could potentially enter through voltage-gated Ca^{2+} channels in the inner segment. We assured that voltage-gated Ca^{2+} channels are inactive by conducting all experiments under voltage clamp at −35 mV holding potential, a condition under which the known Ca^{2+} channels in rod and cone inner segments are inactive (Corey et al., 1984; Maricq and Korenbrot, 1988).

All Ca^{2+} that enters the cell through the CNG channels in the outer segment binds to fura-2. In cones or rods with an inner segment, Ca^{2+} entering the outer segments can flow into the inner segment through the cilium that connects them. Flow between outer and inner segment can be expected for any diffusible molecule. Evidence of this flow is presented in Fig. 3. When 8Br-

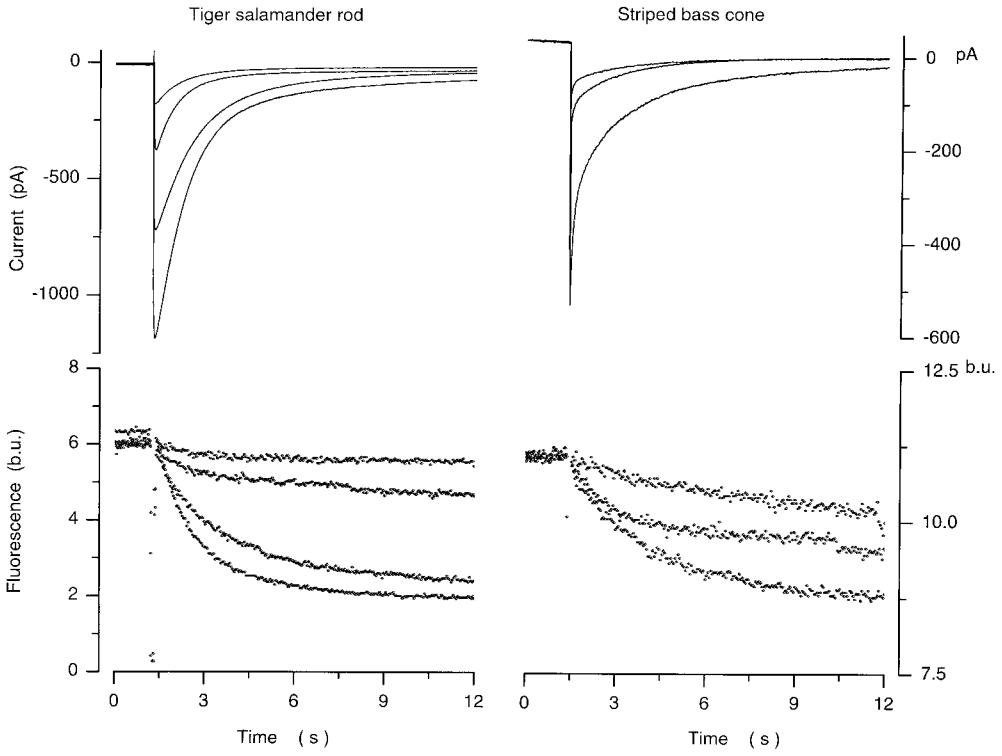

FIGURE 2. Membrane currents and fluorescence measured simultaneously in individual photoreceptor cells loaded with 2 mM fura-2 and 50 μM caged 8Br-cGMP. (Left) Data measured in a dROS from a tiger salamander. The dROS was held at −35 mV and the holding current was −5 pA. Uncaging flashes of varying intensity were presented at various times after achieving whole-cell mode. Each flash caused an inward, transient current and a decrease in fluorescence excited at 380 nm. In between uncaging flashes, both current and fluorescence intensity recovered to their initial values. Peak currents (and time after attaining whole-cell mode) were: 710 pA (12.5 min), 172 pA (15 min), 1,175 pA (25 min), and 362 pA (28 min). (Right) Data measured in a single cone from a striped bass. The cone was held at −35 mV and the holding current was +38 pA. Uncaging flashes also activated inward, transient currents proportional to the intensity of the flash. Peak currents measured (and time after achieving whole-cell mode) were: 179 pA (8.5 min), 79 pA (10.5 min), and 565 pA (12.5 min). Associated with the change in current, there also was a decrease in fluorescence excited at 380 nm. Fluorescence intensity, measured in 50-ms bins, is expressed in bead units. 1 bu is the fluorescence intensity of a single fluorescent bead (Fluoresbrite™ carboxy BB microsphere) measured in the same experiment and under the same conditions used to measure cell fluorescence.

cGMP was released in the inner segment only, by restricting uncaging light to this part of the cell, currents were nonetheless generated in the outer segment. The currents, however, exhibited a delay of a magnitude well predicted for the aqueous diffusion of 8Br-cGMP from the inner segment to the outer segment. To minimize errors that may arise from intracellular Ca^{2+} flow, data in cone photoreceptors were measured by restricting uncaging light to the outer segment alone, but sampling fura-2 fluorescence over the entire cell. Under these conditions, cGMP-dependent Ca^{2+} entry occurs only in the outer segment, but it is fully sampled even if it flows to the inner segment.

In photoreceptor outer segment, entering Ca^{2+} is cleared by a $Na^+/Ca^{2+},K^+$ exchanger and the rate of clearance is faster in cones than in rods (reviewed in Korenbrot, 1995). To investigate whether this transport interferes with P_f determination, we measured currents and fluorescence in a bass single cone in the presence and absence of extracellular Na^+, conditions under which Ca^{2+} clearance through the $Na^+/Ca^{2+},K^+$ exchanger should be active or inactive, respectively. Typical results are illustrated in Fig. 4. Similar observations were made in four other cells. In the presence of normal Ringer, the uncaging flash activated a transient, inward current and caused a decrease in fluorescence. 3 min later, the same cell was superfused with a solution in which all Na^+ was isoosmotically replaced by guanidinium$^+$. Guanidinium$^+$ permeates CNG channels indistinguishably from Na^+ and, therefore, the flash-activated currents, as expected, were nearly identical under both ions. Guanidinium$^+$ does not replace Na^+ in the $Na^+/Ca^{2+},K^+$ exchange, which, therefore, is inactive. The initial decrease in fluorescence was indistinguishable in the presence of the two cations, but ~12 s after the uncaging flash, the time course of fluorescence distinctly diverged. It was nearly stationary in the presence of Na^+, but continued to decline in the presence of guanidinium$^+$ (Fig. 4). It was necessary to return to Na^+ Ringer for the fluorescence to recover its initial value. These results indicate that, in the presence of an active exchanger, 2 mM fura-2 in the cytoplasm retains the entering Ca^{2+} for the first 10 s or so after channel opening. At longer times, a combination of binding saturation of fura-2 and the activity of the exchanger compromises the retention of Ca^{2+} by the fluorescent dye. The method of analysis presented here was applied only to data recorded over the first 6–8 s after the uncaging flash.

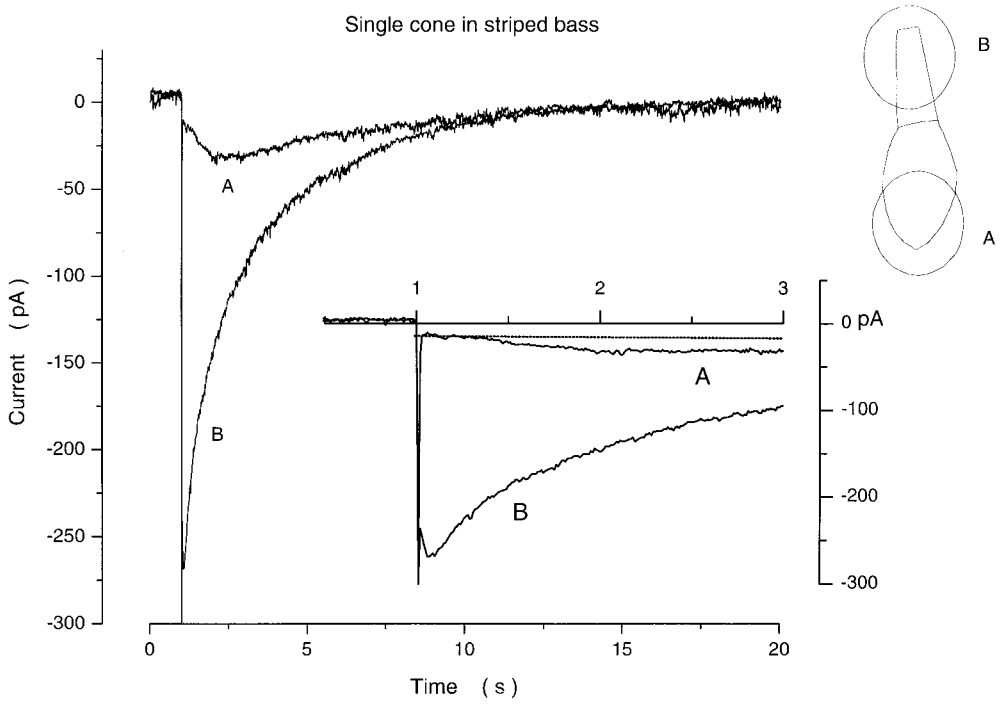

FIGURE 3. Membrane currents measured in a single cone from striped bass loaded with 2 mM fura-2 and 50 μM caged 8Br-cGMP. Superimposed are currents measured in the same cell at −35 mV holding voltage in response to uncaging flashes delivered 4 min (A) or 11 min (B) after achieving whole cell mode. The holding current was +12 pA. Identical flashes were delivered through an aperture that restricted uncaging light to a 20-μm circle centered either on the inner segment (A) or the outer segment (B), approximately as indicated in the drawing (top right). Generating free 8Br-cGMP in the outer segment caused a large, transient inward current without detectable delay relative to the presentation of the flash (B). Generating a similar amount of free 8Br-cGMP in the inner segment also caused an inward current, but smaller in amplitude and slower in time course than that generated by illuminating the outer segment (A). Importantly, this current exhibited a significant delay relative to the moment of presentation of the uncaging flash. The delay was ~400 ms and is consistent with the expected transit time for a small molecule diffusing over a distance of ~20 μm. The inner segment is ~25-μm long.

Fura-2 is at a sufficient concentration to outcompete endogenous buffers. We verified that 2 mM fura-2 is a sufficient concentration by comparing the P_f results obtained in the presence of 1 and 4 mM fura-2. In both rods and cones, P_f data gathered under either concentration were the same (data not shown, but see Frings et al., 2000), indicating that the experimental condition holds. The same conclusion has been reached in previous studies with CNG channels expressed in mammalian cells (Frings et al., 1995; Dzeja et al., 1999).

P_f in Rod Outer Segments of Tiger Salamander

To determine the value of *f*, we measured cGMP-activated changes in current and fluorescence in dROS of tiger salamander in the presence of the solutions listed in Tables I and II. To determine P_f, it was also necessary to measure f_{max}, the value of *f* when $I_T = I_{Ca}$ (Eq. 10). To do so, we carried out experiments using the same protocols used to measure *f*, but we exposed the cells to the solutions listed in Table III. Cells were maintained in normal Ringer's and exposed only for ~60 s to the extracellular test solution to determine f_{max}. Extracellular Na^+ and Mg^{2+} were replaced by the impermeant cation choline, while maintaining Ca^{2+} at the normal 1 mM. Intracellular Mg^{2+} and most of the K^+ ions were also replaced with choline. A small amount of K^+ was retained in the intracellular test solutions to assure that the $Na^+/Ca^{2+},K^+$ exchanger operated in normal, Na^+ Ringer's. At the intracellular K^+ concentration selected and at −35 mV holding voltage, the net K^+ current was zero. Under f_{max} conditions, Ca^{2+} is the only net charge carrier through the CNG channels.

In Fig. 5 are shown typical measurements of *f* and f_{max} in tiger salamander dROS. In the standard Ringer's at −35 mV, the holding current before the uncaging flash was essentially zero and the flash caused a transient inward current and a decrease in fluorescence from its initial value. In the Ringer's, where Ca^{2+} ions are the only net charge carriers, the uncaging flash also generated a transient inward current and a decrease in fluorescence intensity in dROS. Also shown in Fig. 5 are flash-induced changes in fluorescence and the integral of the current changes. These two data sets superimpose over a span of ~5 s after the flash (Fig. 5, bottom). Superimposition is evidence that the conditions necessary to calculate *f* (see above) are met over this restricted time span. We determined the singular value of *f*, the ratio of the change in fluorescence to the current integral only over this restricted time span (*f*, bu/pC).

The mean peak photocurrent amplitude in tiger salamander rods is ~70 pA (Miller and Korenbrot, 1994). To determine the value of P_f under conditions similar to those expected in the functional retina, we

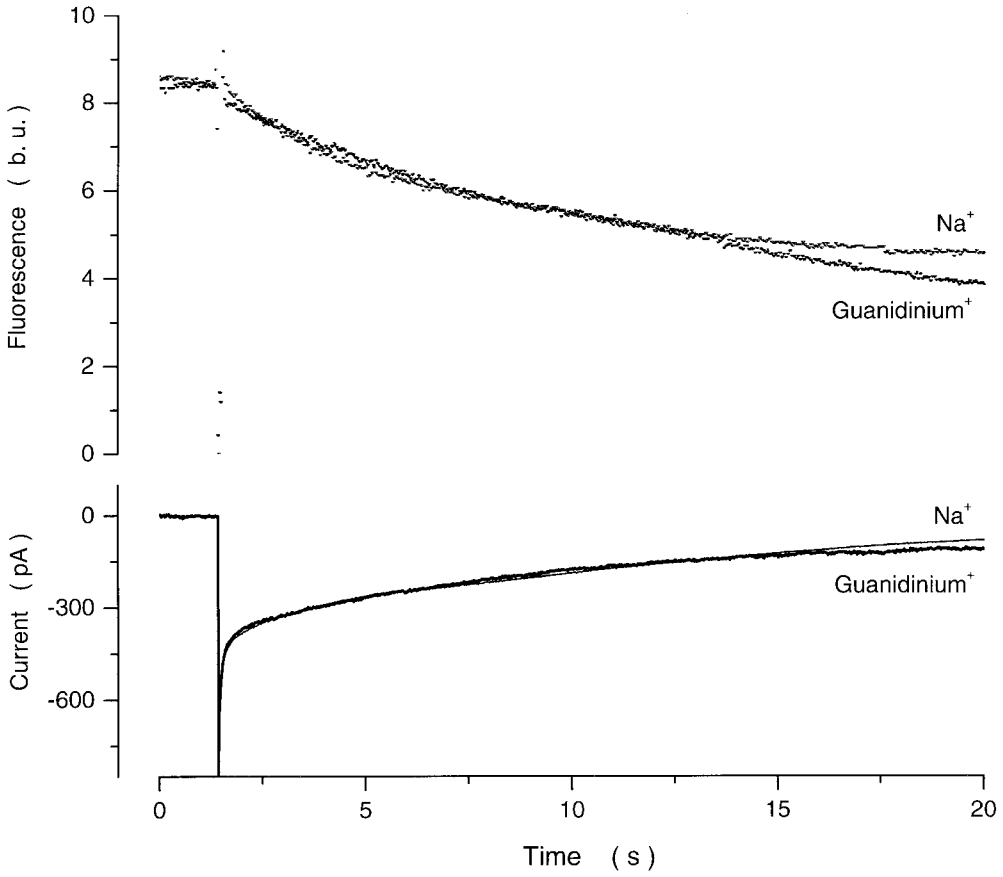

FIGURE 4. Membrane currents and fluorescence measured simultaneously in a single cone from striped bass loaded with 2 mM fura-2 and 50 μM caged 8Br-cGMP. Superimposed are currents measured in the same cell at −35 mV holding voltage in response to identical uncaging flashes delivered 6.5 min (Na^+) or 8.5 min (Guanidinium$^+$) after achieving whole-cell mode. The Na^+ tracing was measured in the presence of the normal Ringer's solution, while the Guanidinium$^+$ tracing was measured starting 15 s after switching the medium superfusing the cell from normal Ringer's to one in which Na^+ was iso-osmotically replaced by guanidinium$^+$. The holding current in the presence of Na^+ was +22 pA, but it changed to −44 pA in the presence of guanidinium$^+$. Currents were corrected to have their holding value be zero preceding the flash. Fluorescence intensity before the flash was the same. The flash-activated currents under both ionic conditions were essentially indistinguishable. The associated decrease in fluorescence were also indistinguishable at first, but began to diverge ~12 s after the flash.

restricted analysis to data sets in which uncaging flashes generated peak current amplitudes ≤200 pA, with a mean value of 115 ± 53. The average value of f_{max} was 0.0112 ± 0.0019 bu/pC (13 measurements in eight different cells, range 0.0101–0.0130). The average value of f was 0.00238 ± 0.0009 bu/pC (n = 17). Hence, under these conditions, the average value of P_f (Eq. 11) in tiger salamander rods is: 0.21 ± 0.01

We also measured P_f in dROS of gecko because the Ca^{2+} homeostasis of this organelle has been carefully and thoroughly studied (Gray-Keller and Detwiler, 1994; Gray-Keller et al., 1999). We studied this species less extensively than others and we pooled data measured in cells over a much wider range of peak current amplitudes. For currents between 210 and 1,048 pA in peak amplitude, the average f value was 0.0044 ± 0.0012 bu/pC (n = 4). Given f_{max} of 0.022 for these cells, the average value of P_f in gecko rods is 0.19 ± 0.05.

P_f in Single Cones of Striped Bass

In Fig. 6 are shown typical measurements of f and f_{max} in single cones of striped bass. Shown are electrical and photometric data both in standard Ringers solution and in one designed to have Ca^{2+} ions as the only net charge carrier. The experimental data are qualitatively similar to that in dROS, uncaging flashes cause a transient inward current and a decrease in fluorescence. We analyzed the experimental data to determine the values of f and f_{max} as described above. For currents <200 pA in peak amplitude, the average value of f_{max} was 0.0098 ± 0.0014 bu/pC (range 0.008–0.0125, n = 9). The average value of f was 0.0032 ± 0.0011 bu/pC (n = 40). Hence, under these conditions, the average value of P_f (Eq. 11) in striped bass single cones is 0.33 ± 0.02.

P_f in Single Cones and Rods of Catfish

The two species described above, tiger salamander and striped bass, are the ones in which most of the electri-

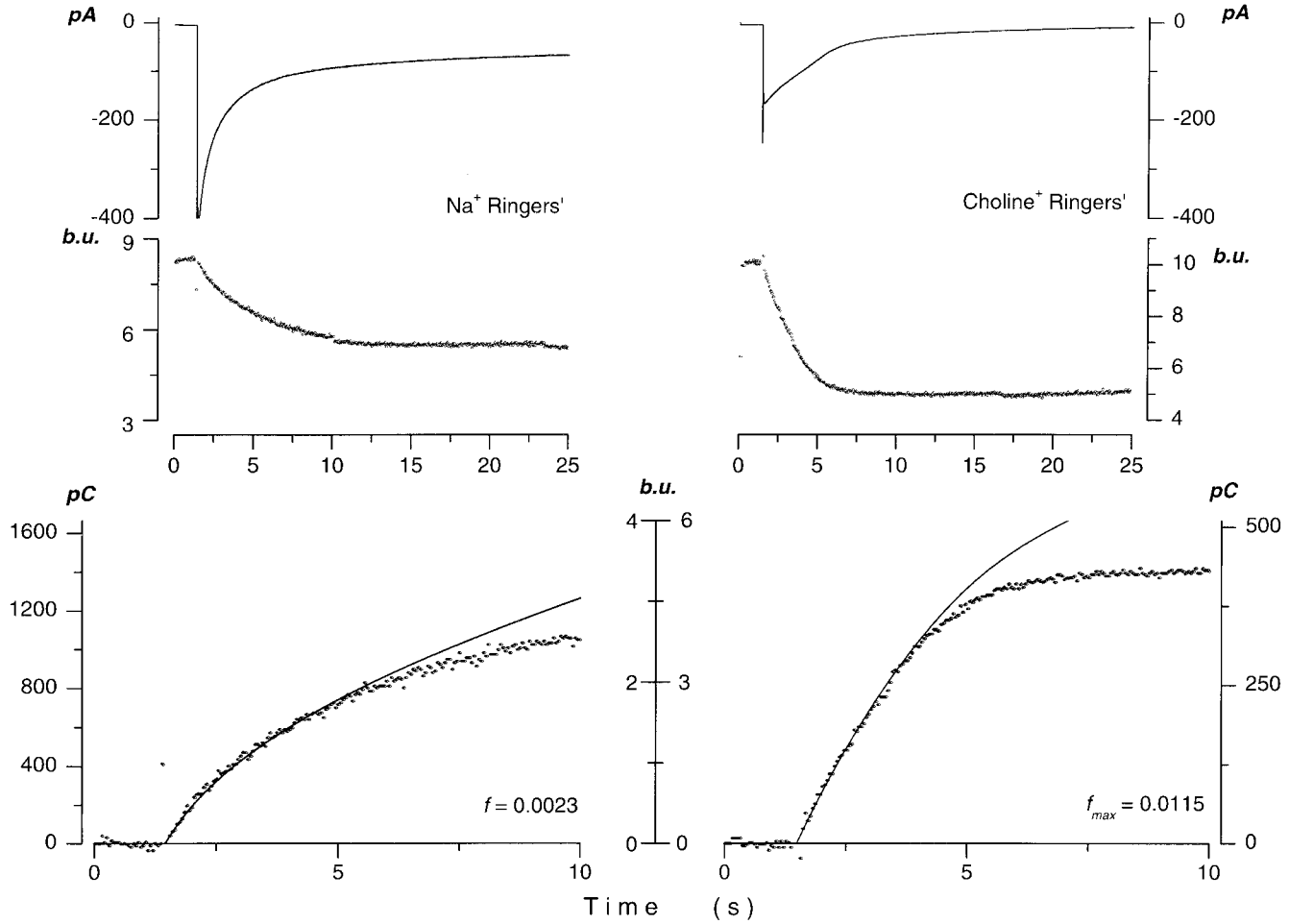

FIGURE 5. Determination of the values of f and f_{max} in detached rod outer segments from tiger salamander. (Left and right) Records from different cells. (Top) Membrane currents and fluorescence measured simultaneously in rods loaded with 2 mM fura-2 and 50 μM caged 8Br-cGMP. Uncaging flashes activated transient, inward currents and a decrease in cell fluorescence. To analyze the data, currents were integrated over the time shown and the resulting charge is shown as a continuous line (pC, bottom). The flash-activated change in fluorescence was shifted to assign its average holding value preceding the flash to be zero (bottom). f is the ratio of the change in fluorescence to the integral of the change in current, measured over the time interval where the two scaled parameters superimpose fully. The value of f was measured under the normal physiological solution (Na^+ Ringers). The value of f measured under experimental conditions designed to have Ca^{2+} be the exclusive, net charge carrier through the CNG ion channels (Choline$^+$ Ringers), is defined as f_{max}. For the rods shown, under Na^+ Ringers, the holding current was −4 pA, the peak current was 408 pA measured 10 min after achieving whole cell mode, and f was 0.00237. Under Choline$^+$ Ringers, the holding current was −4 pA, the peak current was 159 pA measured 7 min after achieving whole cell mode, and f_{max} was 0.01154.

cal studies of ion selectivity have been conducted. The rod versus cone differences described, however, could represent differences between species, rather than between photoreceptor types. This is unlikely since rod/cone differences are also found in alpha subunit channels of bovine photoreceptors (Frings et al., 1995; Dzeja et al., 1999). Nonetheless, we investigated the value of P_f in rods and cones of the same species.

In Fig. 7 are shown typical measurements in rods and cones of catfish. In this species, unlike tiger salamander or gecko, the detached rod outer segment includes a small portion of the cell's ellipsoid. Consequently, at −35 mV, the holding current preceding the uncaging flash was outward both in the dROS and the single cones. In both cell types, the uncaging flash caused an inward current and a decrease in fluorescence. For uncaging flashes of the same intensity, the amplitude of the inward currents (and its concomitant change in fluorescence) was always smaller in cones than in rods. This almost certainly reflects the fact that the sensitivity for cGMP is higher in channels of rods than in those of cones (Haynes and Yau, 1990; Rebrik and Korenbrot, 1998).

We determined the values of f (Fig. 7) and f_{max} (data not shown) for rods and cones of the catfish.

Cones. For currents <75 pA in peak amplitude (range 30–75 pA), the average value of f_{max} was 0.0087 ± 0.0031 bu/pC (nine determinations in six cells). For currents <200 pA in peak amplitude, the average f

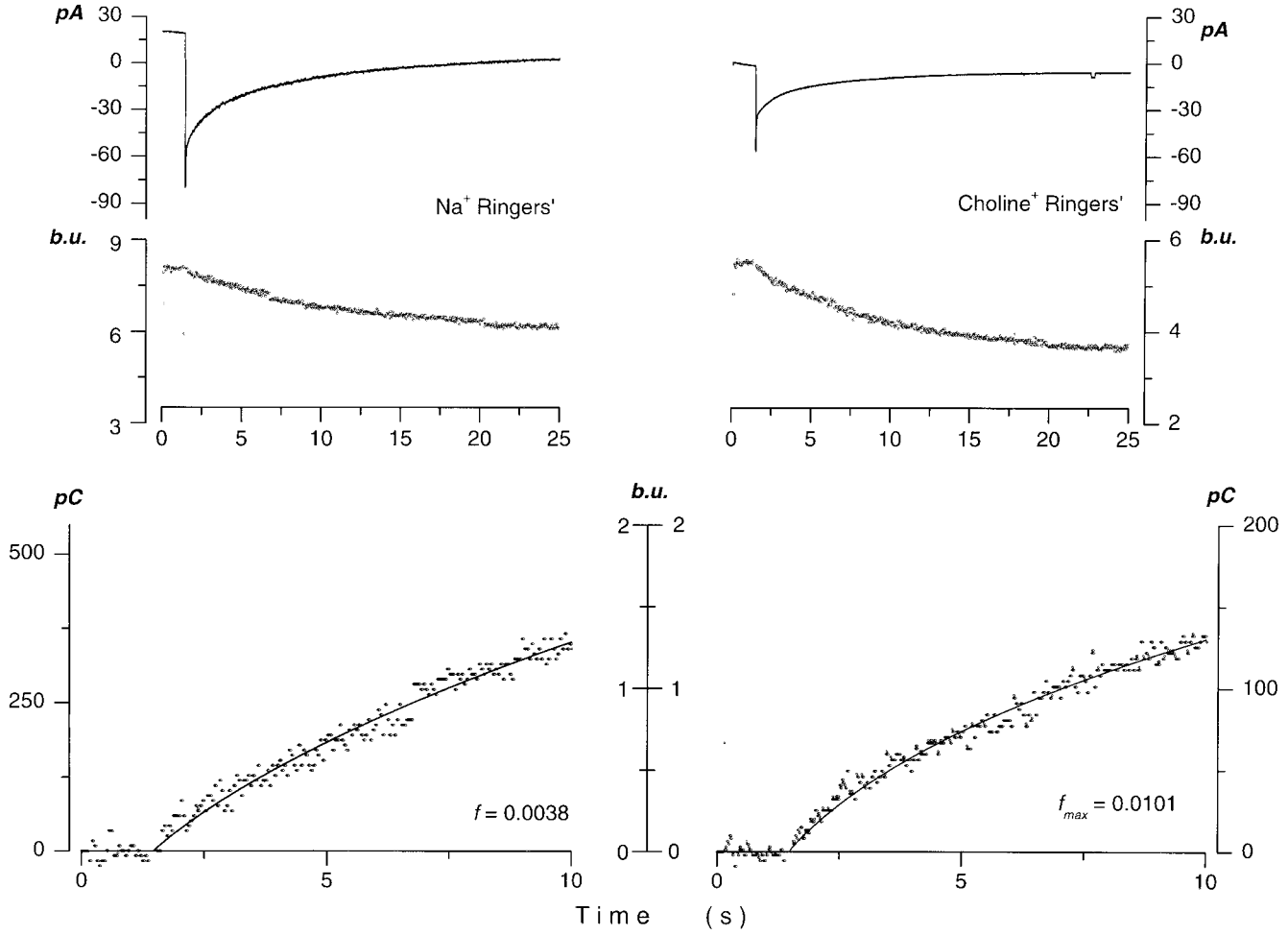

FIGURE 6. Determination of the values of f and f_{max} in single cones from striped bass. (Top) Membrane currents and fluorescence measured simultaneously in cones loaded with 2 mM fura-2 and 50 μM caged 8Br-cGMP. Uncaging flashes activated transient, inward currents and a decrease in cell fluorescence. To analyze the data, both currents and fluorescence were shifted to have their average holding value be zero preceding the uncaging flash. Currents were integrated starting from this zero value (bottom, continuous line) and the integral was scaled and superimposed on the flash-generated change in fluorescence (bottom). f is the ratio of the current integral to the fluorescence over the time interval that the two superimpose. In different cells, we measured f under physiologic solutions (Na^+ Ringers) and f_{max} under experimental conditions designed to have Ca^{2+} be the exclusive, net charge carrier through the CNG ion channels ($Choline^+$ Ringers). For the cones shown, under Na^+ Ringers, the holding current was 22 pA, the peak current was 75 pA measured 9 min after achieving whole cell mode, and f was 0.00382. Under $Choline^+$ Ringers, the holding current was 0 pA, the peak current was 56 pA measured 4 min after achieving whole cell mode, and f_{max} was 0.01017.

value was 0.00295 ± 0.0013 bu/pC (17 determinations in 11 cells). Under these conditions, the average value of P_f was 0.34 ± 0.06.

Rods. For currents <50 pA in peak amplitude (range 13–40 pA), the average value of f_{max} was 0.0124 ± 0.0028 bu/pC (seven determinations in four cells). For currents <220 pA in peak amplitude, the average f value was 0.00174 ± 0.0005 bu/pC (19 determinations in 12 cells). Under these conditions, the average value of P_f was 0.14 ± 0.01.

The values of P_f at −35 mV holding voltage, for cGMP-dependent currents <200 pA in amplitude and in the presence of 1 mM external Ca^{2+} for the species studied here, are compared in Fig. 8. The differences in Ca^{2+} fractional current between rods and cones are thus features preserved across species.

Interaction between Ca^{2+} and CNG Channels Are Reflected in the Value of P_f and Differs Between Channels of Rods and Cones

We measured the current and fluorescence changes caused by identical flashes delivered to the same cell bathed in varying amounts of Ca^{2+} (Table I). Cells were superfused with test solution beginning 15 s before the flash and for the course of the measurement (30 s). Otherwise, cells were maintained in the normal Ringer's. We waited 2–3 min between flashes, time sufficient for cells to recover to their starting conditions. We analyzed only data in which these starting values differed by <10%.

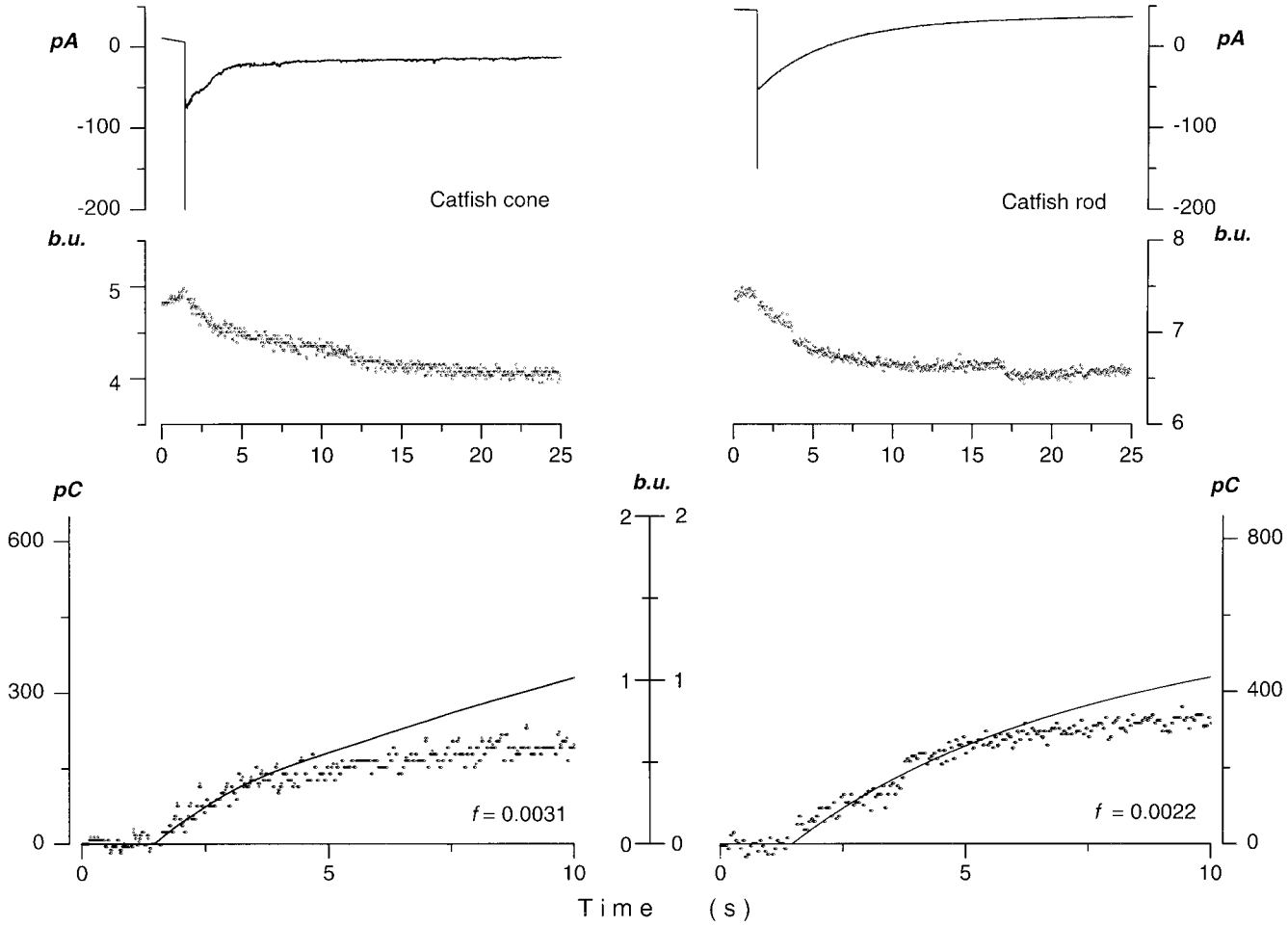

FIGURE 7. Determination of the values of f in single cones and rods from catfish under physiologic solutions. (Top) Membrane currents and fluorescence measured simultaneously in photoreceptors loaded with 2 mM fura-2 and 50 μM caged 8Br-cGMP. Uncaging flashes activated transient, inward currents and a decrease in cell fluorescence. To analyze the data, both currents and fluorescence were shifted to have their average holding value be zero preceding the uncaging flash (bottom). Currents were integrated starting from this zero value (bottom, continuous line) and the integral was scaled and superimposed on the flash-generated change in fluorescence. f is the ratio of the current integral to the fluorescence, over the time interval that the two superimpose. For the cone shown, the holding current was 11 pA, the peak current was 85 pA measured 4 min after achieving whole cell mode, and f was 0.0031. For the rod shown, the holding current was 45 pA, the peak current was 97 pA measured 11 min after achieving whole cell mode and f was 0.0022.

We tested various Ca^{2+} concentrations in random sequence, but always started at the normal 1 mM Ca^{2+}.

In Fig. 9 are shown typical data measured in striped bass single cones and tiger salamander dROS. We illustrate fluorescence changes and the integral of the current scaled to optimally fit the changes in fluorescence. For both photoreceptor types, the data shown were measured at 3-min intervals in the same cell bathed with varying external Ca^{2+} concentrations. The signal-to-noise ratio in the photometric cone data is significantly less than in those of rods because bass cone outer segments are only about one tenth the volume of the tiger salamander's rod outer segments. In cones, the average f values we measured were: at 0.5 mM Ca^{2+}, 0.00129 ± 0.00018; at 1 mM Ca^{2+}, 0.00295 ± 0.00049; at 1.5 mM Ca^{2+}, 0.00383 ± 0.00113; at 2 mM Ca^{2+}, 0.00421 ± 0.0015; at 2.5 mM Ca^{2+}, 0.00518 ± 0.0021; and at 5 mM Ca^{2+}, 0.00952 ± 0.00603. Data were measured in a total of 10 cells, with any one concentration sampled in 3–10 cells. Thus, fractional Ca^{2+} current increased steeply with Ca^{2+} concentration. The dependence of P_f on Ca^{2+} was well described by the Michaelis-Menten function:

$$P_f(\mathrm{Ca}) = \frac{\mathrm{Ca}}{\mathrm{Ca} + K\mathrm{Ca}}. \quad (12)$$

KCa is the value at which $P_f = 0.5$. We obtained the best fit to the mean of the data with KCa = 1.98 mM.

In rods, the fractional Ca^{2+} current also increased with external Ca^{2+}, but much less steeply than in cones and, even at 10 mM, external Ca^{2+} carries only about half the current (Fig. 9). The average f values we mea-

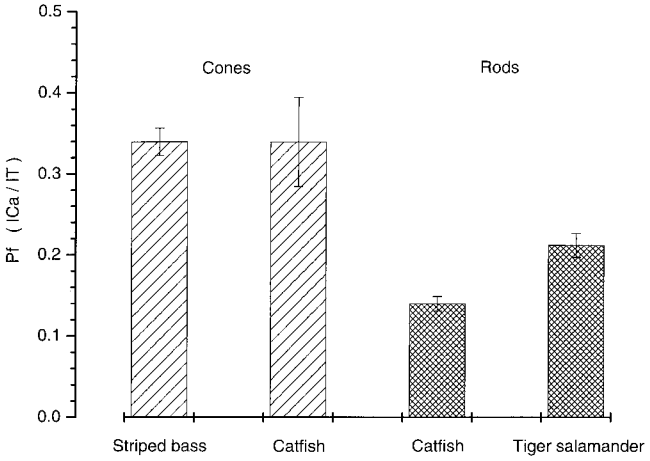

FIGURE 8. Mean (± SD) of the fractional Ca^{2+} flux (P_f) measured in rods and cones of several species under normal Ringers solutions. The data were pooled from measurements in cells held at −35 mV, in the presence of 1 mM external Ca^{2+} and for cGMP-dependent currents ≤200 pA in peak current amplitude.

sured were: at 1 mM Ca^{2+}, 0.00286 ± 0.000883; at 2.5 mM Ca^{2+}, 0.003812 ± 0.00098; at 5 mM Ca^{2+}, 0.005713 ± 0.004314; and at 10 mM Ca^{2+}, 0.00668 ± 0.000496. Data were measured in a total of nine cells, with any one concentration sampled in four to nine cells. We note that in this data set, the mean value of P_f at 1 mM Ca^{2+} was 0.25 ± 0.043. This value is slightly larger than the mean value presented above because the data set included peak 8Br-cGMP-dependent current of amplitude ≤1,000 pA, with a mean value of 454 ± 347 pA. The mean value of P_f is smaller for currents ≤200 pA because selectivity is linked to gating in rod CNG channels (Hackos and Korenbrot, 1999). The best fit of the Michaelis-Menten function (Eq. 12) to the mean of the rod data was obtained with KCa = 4.96 mM (Fig. 9).

DISCUSSION

We have directly measured the fraction of the cGMP-gated current carried by Ca^{2+} in the outer segment of intact rods and cones. Ca^{2+} carries 14–20% of the dark current in rods and 32–34% in cones. The differences in fractional Ca^{2+} flux between rods and cones are maintained across several species.

Our results in rods are similar to those of indirect measurements previously reported by others, and based on an analysis of the current generated by the electrogenic transport activity of $Na^+/Ca^{2+},K^+$ exchangers in the outer segment membrane (Nakatani and Yau, 1988; Lagnado et al., 1992; Gray-Keller and Detwiler, 1994; Younger et al., 1996). Such analyses require the unambiguous separation of the exchanger current from the photocurrent, as well as assumptions about transport stoichiometry. The indirect studies have set the value of P_f in rods anywhere between 0.10 and 0.18. The similarity of present and past results in rods confirms the accuracy of the indirect method and extends the observation to several species.

Our results in cones are in quantitative disagreement with those reported by Perry and McNaughton (1991), based on analysis of the electrogenic exchanger currents in tiger salamander cones. Perry and McNaughton (1991) correctly recognized that the fraction of the dark current carried by Ca^{2+} current is higher in cones than in rods. Their estimate of this fraction, however, is smaller than the results we have found. They estimated that P_f is 0.12 in rods and 0.21 in cones. This difference likely reflects the uncertainty in separating the exchanger from the conductive currents. The exchanger current in rods of lower vertebrates decays with an exponential time course of several hundred milliseconds or seconds time constant (Nakatani and Yau, 1988; Lagnado et al., 1992; Gray-Keller and Detwiler, 1994; Younger et al., 1996). In cones, in contrast, the exponential decay of the exchanger current has a time constant of tens of milliseconds duration (Hestrin and Korenbrot, 1990; Perry and McNaughton, 1991).

Previous electrical studies had established that the selectivity of Ca^{2+} over Na^+, PCa/PNa, measured from reversal potentials is higher in CNG channels of cones than in those of rods (Frings et al., 1995; Picones and Korenbrot, 1995). These measurements, however, are conducted under simple ionic solutions, with only Ca^{2+} and Na^+ present. Extending them to determine the fractional Ca^{2+} flux under normal physiological solutions is complex and requires application of a specific model of ion permeation. Wells and Tanaka (1997) have developed a plausible model based on Eyring rate theory that successfully simulates PCa/PNa, I-V curves and the Ca^{2+} fractional flux in rod CNG channels. The model presumes the existence of three barriers, two wells, and four sites that interact electrostatically (each for Na^+, K^+ Ca^{2+} and Mg^{2+}). Similar but less elaborate models were first formulated and analyzed by Zimmerman and Baylor (1992). A comparably complete computation has not been reported for cone CNG channels. However, a simpler Eyring-type model consisting of one barrier and two wells has been successfully used to analyze monovalent cation selectivity in cone CNG channels (Picones and Korenbrot, 1992; Haynes, 1995).

An indirect conclusion supported by our results is that strong buffering sites for cyclic nucleotides operate in intact rod and cone outer segments of all species tested. The sites are relatively fast in kinetics, their K_d is high and they are active in the cyclic nucleotide concentration range expected under normal operating conditions in the cell. Biochemical analysis suggests that, in rods, the cGMP binding sites are noncatalytic sites on phosphodiesterase (Cote and Brunnock, 1993). The sites are not functionally different in rods and cones.

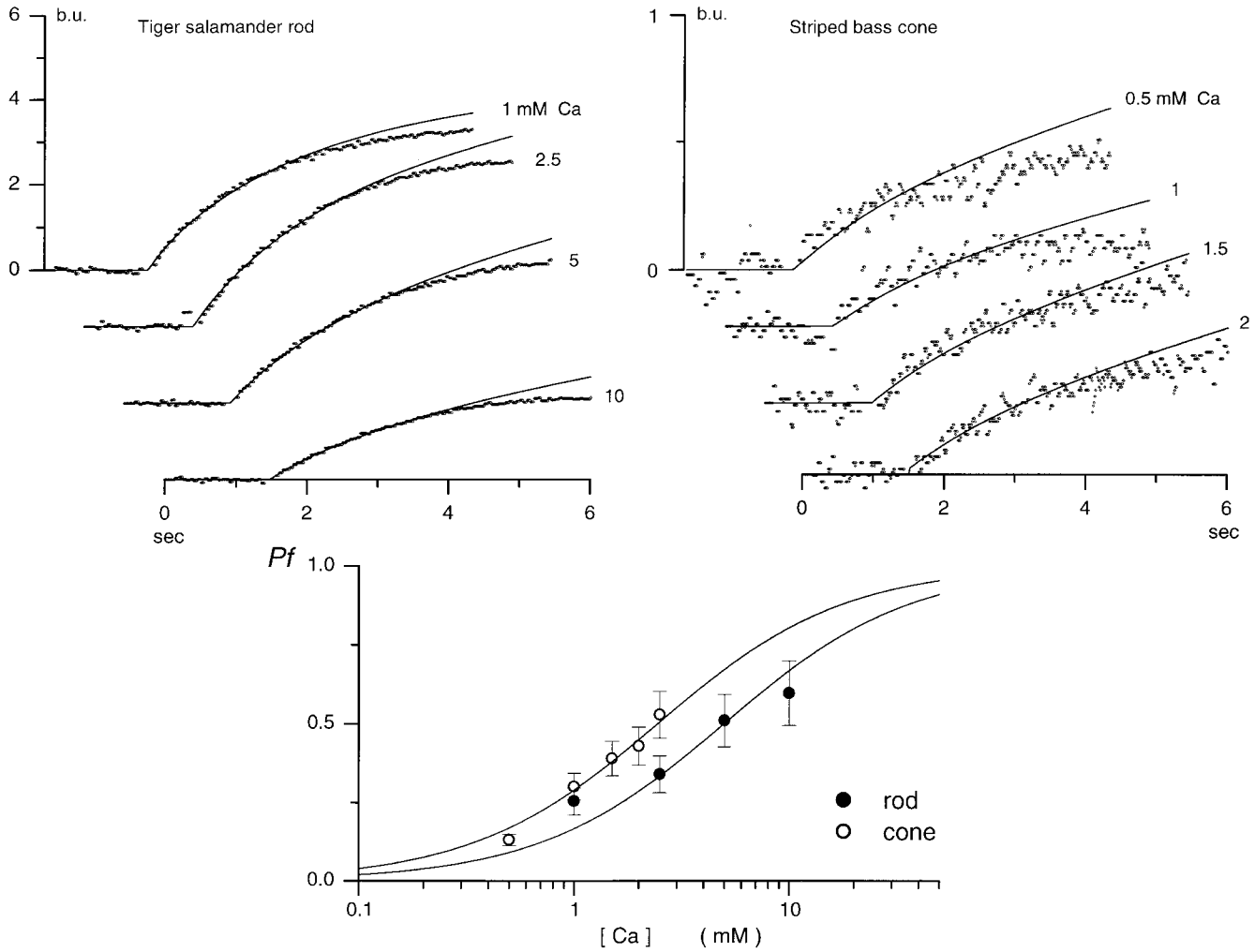

FIGURE 9. Dependence of fractional Ca^{2+} flux (P_f) on external Ca^{2+} concentration. (Top) Data measured in a tiger salamander dROS (left) and a striped bass single cone (right). For each photoreceptor type, data shown were measured in the same cell in the presence of Ringers containing different Ca^{2+} concentrations, as labeled. Shown are the flash-activated changes in fluorescence and the integral of the flash-activated changes in current (continuous line) scaled to match. For the dROS shown, Ihold throughout was −4 pA. At 1 mM Ca^{2+} (4 min after achieving whole-cell mode), Ipeak = 690 pA; at 2.5 mM Ca^{2+} (6 min), Ipeak = 354; at 5 mM Ca^{2+} (8 min), Ipeak = 300. For the cone shown, at 1 mM Ca^{2+} (4 min), Ihold = 20 pA, Ipeak = 162 pA; at 1.5 mM Ca^{2+} (8 min), Ihold = 12 pA, Ipeak = 97 pA; at 2 mM Ca^{2+} (10 min), Ihold = 20 pA, Ipeak = 162 pA. (Bottom) Mean value of P_f as a function of Ca^{2+}. The continuous line is an optimum fit to the experimental data of the Michaelis-Menten function (Eq. 12). For cones, the best fit was obtained with KCa = 1.98 mM, and for rods KCa = 4.96 mM.

There are significant physiological consequences to accurately knowing the value of P_f. Cytoplasmic Ca^{2+} homeostasis in the photoreceptor outer segment arises from the dynamic balance of influx, efflux, and buffering by endogenous sites, with no role recognized for transport in or out of intracellular compartments. Knowing the value of P_f, therefore, is crucial to understanding Ca^{2+} dynamics. This is made particularly clear by computational models developed to explain in molecular detail the phototransduction process. Particularly detailed and thorough models have been put forward (Forti et al.; 1989; Sneyd and Tranchina, 1989; Torre et al., 1990; Nikonov et al., 1998). Every one of these models includes an explicit term for P_f, and the value assigned to this parameter strongly affects the performance of the model.

The difference in P_f between rod and cone channels implies that light-dependent changes in Ca^{2+} concentration caused by equal amplitude currents will be larger in cones than in rods. This fact, added to the known difference in the clearance rate of Ca^{2+} from the outer segment indicates that, for a given current response, Ca^{2+} concentration changes will be larger and faster in cones than in rods. These differences contribute to explaining the dissimilarity in the photosensitivity, kinetics, and light- and dark-adaptation characteristics of the two photoreceptor types.

Differences in P_f between rod and cone channels reflect differences in the molecular interaction between the cation and the channel protein. Seifert et al. (1999) studied homomeric channels formed from α subunits of CNG channels cloned from olfactory neurons, rod, and cone photoreceptors and *Drosophila*. They discovered that the interaction between extracellular Ca^{2+} and the channels differs among channels cloned from different cell types (rod versus cone versus olfactory), but not among channels cloned from the same cell type in different species (bovine versus chicken versus rabbit). Again, a unique CNG channel structure/function is associated with a specific cell type, regardless of the animal species in which the cell is found.

Mutagenesis analysis has demonstrated than in recombinant homomeric alpha CNG channels, Ca^{2+} interacts with a glutamate residue within the pore loop of the channel (E363) (Root and Mackinnon, 1993; Eismann et al., 1994). Although the same residue exists in the pore of all CNG alpha channels, the thermodynamics of the interaction between Ca^{2+} and glutamate E363 differs among CNG channels. For example, the extracellular Ca^{2+} concentration that blocks channel conductance by 50% at −70 mV is 7 μM in rods, but 68 μM in cones (Seifert et al., 1999). Thus, structural features of E363 alone cannot explain the characteristics of the interaction between Ca^{2+} and the CNG channels. Recent work has demonstrated that the Ca^{2+}/E363 interaction changes with the state of protonation of the residue, which, in turn, is controlled by structural features of the regions of the protein adjacent to the pore, the S5 and S6 loops (Seifert et al., 1999). The S5-pore-S6 "structural module" differs among recombinant alpha channels depending on the cellular source of the cDNA (Seifert et al., 1999).

The molecular view of the interaction between Ca^{2+} and the S5-pore-S6 structural module obtained from experiments with recombinant homomeric alpha CNG channels cannot simply be extended to the structure of the native photoreceptor channels. Native channels in both rods and cones are formed from alpha and beta subunits. Rod channels are formed by two alpha and two beta subunits, although the sequence of these subunits is controversial (Shammat and Gordon, 1999; He et al., 2000). Two striking differences exist between native and recombinant alpha channels with respect to their Ca^{2+} fractional currents. (a) In the presence of 1 mM external Ca^{2+}, P_f in native cone channels is about twice that in rods, but in alpha recombinant channels this is reversed: P_f in rods is about three times larger than that in cones. (b) The Ca^{2+} dependence of P_f is extremely steep in rod alpha recombinant channels, but remarkably shallow in native rod channels. In recombinant channels, the Ca^{2+} concentration at which $P_f = 0.5$ is 0.4 mM and P_f is essentially 1 when Ca is only 1 mM (Dzeja et al., 1999). In the native channel, P_f is 0.2 at 1 mM Ca^{2+} and even when Ca^{2+} is 10 mM, P_f is still only ∼0.5.

A structural understanding of the differences between recombinant alpha and native channels is not at hand, but, if we extend the information gained from the structural studies of Seifert et al. (1999), the functional differences likely reflect differences in the dielectric environment surrounding the pore glutamate. Differences in dielectric environment can arise from two possible sources or their combination. The obvious first possibility is that the beta subunits, which have a glycine instead of a glutamate in the pore loop, create a pore sufficiently unlike that in alpha channels as to explain the difference. A second possibility is that the dielectric environment is changed by Mg^{2+} ions. The results reported here were all measured in the presence of 1 mM external Mg^{2+} and 0.5 mM free cytoplasmic Mg^{2+}. The studies of alpha recombinant channels were conducted in the absence of external Mg^{2+} and with 0.27 mM free cytoplasmic Mg^{2+} (Dzeja et al., 1999). Because the channels bind Mg^{2+} almost as well as Ca^{2+}, the presence of Mg^{2+} must influence the interaction between Ca^{2+} and the channel (Wells and Tanaka, 1997). The role of these two possible mechanisms needs to be resolved experimentally.

It is notable that, whereas the dependence of P_f on outside Ca^{2+} differs significantly between native and recombinant rod channels, this is not the case for cone channels. In both native and recombinant cone channels, the Michaelis-Menten function describes well the dependence of P_f on Ca^{2+}, with KCa = 1.38 mM in alpha recombinant channels (Dzeja et al., 1999) and KCa = 1.98 mM in native ones. This characteristic of the channels is similar despite the fact that measurements were conducted in the absence of Mg^{2+} in recombinant proteins and with 1 mM outside Mg^{2+} in the native cells. If the presence of beta subunits is important in defining the interaction of divalent cations with native channels, our results suggest that the alpha/beta subunit interactions differ in rods and cones. Future work should provide information on the mechanisms of this difference.

APPENDIX

We investigated possible mechanisms to explain the surprisingly rapid decay of the outer segment current generated by uncaging 8Br-cGMP (Fig. 2). If 8Br-cGMP were not processed within the outer segment, it would be reasonable to expect a slow decay in current after the uncaging flash due to equilibration of freed 8Br-cGMP between cytoplasm and electrode lumen. To determine the rate of this equilibration, we used tight-seal electrodes filled with the usual solution (Table II) containing, in addition, 30 μM 8Br-cGMP, and we moni-

tored the membrane current after membrane rupture to attain whole-cell mode. Fig. 10 illustrates a typical result in bass single cones at −35-mV holding voltage. After membrane rupture, an inward current developed without detectable delay that reached a maximum in ~52 s. In eight different cells, the mean time to the maximum was 73.6 ± 22.3 s. Since current decay after an uncaging flash is much, much faster (above), its time course cannot be explained by the rate of cell/electrode equilibration.

Rapid current decay could reflect hydrolysis of free 8Br-cGMP by phosphodiesterase (PDE) activated by the uncaging flash. This is plausible because, while 8Br-cGMP is ~100-fold less effective than cGMP as a substrate of rod PDE (Zimmerman et al., 1985), it can, if present at a sufficiently high concentration, be hydrolyzed by activated PDE. Indeed, bright lights generate photocurrents in rods loaded with high concentrations of 8Br-cGMP (0.5–1 mM) (Cameron and Pugh, 1990). To test whether current inactivation reflects 8Br-cGMP hydrolysis by PDE, we conducted two control experiments. In the first one, we measured in single cones the current generated by uncaging cGMP in the continuous presence of 0.1 mM 3-isobutyl-1-methylxanthine (IBMX), an effective blocker of cone PDE (Gillespie and Beavo, 1989). The current rapidly reached a peak and, in spite of the presence of IBMX, it decayed with an exponential time course similar to that measured in the absence of the blocker (Fig. 10). In a second control experiment, we tested whether the uncaging flash generated a photoresponse in single cones loaded with 15 μM 8Br-cGMP. We do not know the exact concentration of free 8Br-cGMP generated by the uncaging flash, but considering that $K_{1/2}$, the nucleotide concentration that half activates the maximum CNG current in the intact cone in the absence of Ca^{2+}, is ~15 μM (Rebrik and Korenbrot, 1998), the concentration necessary to generate 200 pA current is ~5.5 μM. Even in the presence of 15 μM 8Br-cGMP, the flash did not cause a photocurrent (Fig. 10). We can, therefore, reject the hypothesis that current decay is caused by 8Br-cGMP hydrolysis.

Ca^{2+} modulates ligand sensitivity of CNG channels in both rods (Hsu and Molday, 1993; Gordon et al., 1995; Sagoo and Lagnado, 1996; Bauer, 1996) and cones (Rebrik and Korenbrot, 1998). Therefore, it is possible that current decay reflects a decrease in CNG channel sensitivity to free ligand, caused by a rise in cytoplasmic Ca^{2+} associated with the enhanced current. Such modulation, however, is unlikely to occur under our experimental conditions because changes in cytoplasmic free

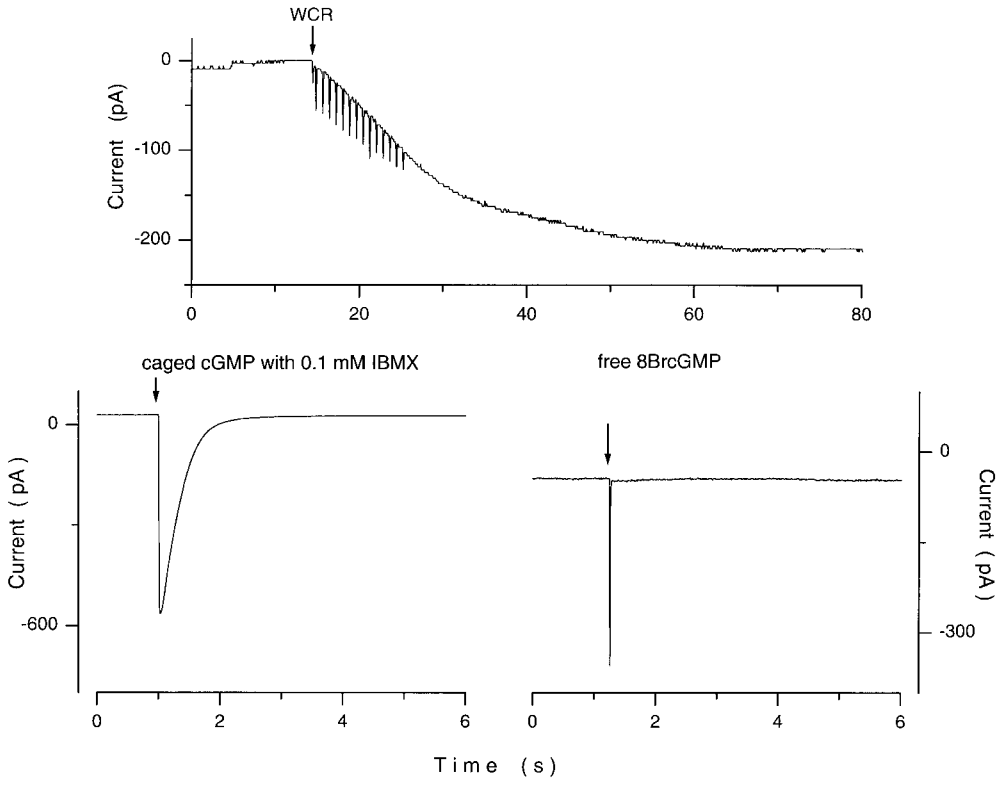

FIGURE 10. (Top) Rate of 8Br-cGMP loading of a bass single cone by equilibration between the cell and the lumen of a tight-seal electrode. (WCR) The moment the membrane under the electrode tip was ruptured. Inward current (at −35 mV holding voltage) is activated by the continuously rising concentration of 8Br-cGMP in the cone outer segment. A maximum current is reached in ~52 s. The transients on the membrane current at the earliest times after attaining WCR are currents generated by 200-ms duration, 5-mV voltage steps applied to ascertain cell integrity. (Bottom) Hydrolysis of free cyclic nucleotide by PDE does not explain the decay of current generated by uncaging light flashes. (Bottom, left) Membrane current measured at −35 mV in a single cone loaded with 50 μM caged cGMP in the presence of 0.1 mM IBMX added to the bathing Ringers solution. A brief, bright flash uncaged the nucleotide and caused an inward current that reached peak in ~30 ms, and then decayed exponentially with a 0.24 s time constant. The same behavior is observed in the absence of the PDE blocker. (Bottom, right) Membrane current measured at −35 mV in a single cone loaded with 15 μM free 8Br-cGMP. An uncaging flash was delivered at the moment indicated by the arrow. The flash caused a rapid transient, an artifact due to the discharge of the Xenon lamp, but the current was otherwise unchanged, indicating that light-activated PDE did not hydrolyze 8Br-cGMP at this concentration.

Ca^{2+} are vanishingly small in the first 6–8 s after the uncaging flash due to the presence of 2 mM fura-2.

We propose that the rapid current decline arises from binding of free 8Br-cGMP to specific sites in rod and cone outer segments. The existence of cGMP-binding sites in rod outer segments has been inferred from analysis of cGMP diffusion kinetics (Olson and Pugh, 1993; Koutalos et al., 1995) and measured biochemically (Cote and Brunnock, 1993). These sites are presumed to be the known noncatalytic nucleotide binding sites on PDE molecules (Hebert et al., 1998). To test this hypothesis, we carried out a competition experiment in the intact cell. The noncatalytic binding site in the rod PDE binds cIMP (3′-5′ cyclic inosine monophosphate) with ~20-fold higher affinity than 8Br-cGMP (Hebert et al., 1998). On the other hand, the ligand sensitivity of the rod CNG channels for cIMP is ~0.006-fold that for 8Br-cGMP. $K_{1/2}$ is ~8 μM for 8Br-cGMP, but ~1.2 mM for cIMP (Tanaka et al., 1989). Based on these quantities, simple calculations indicate that 20 μM cIMP should not activate the CNG channels (<0.003%), but should significantly reduce binding of free 8Br-cGMP to the PDE. If 8Br-cGMP binding is reduced by cIMP, this should be apparent by a slowdown in the kinetics of binding of 8Br-cGMP in the presence of cIMP, when compared to the kinetics of binding in the absence of cIMP. This is indeed the case (Fig. 11).

We measured in tiger salamander dROS the current activated by uncaging 8Br-cGMP in the presence of 20 μM cIMP. We filled tight-seal electrodes with the standard solution containing caged 8Br-cGMP and fura-2 (Table II) with an additional 20 μM cIMP. The mean holding current was unaffected, indicating that, as expected, cIMP at this concentration did not activate CNG channels. An uncaging flash caused a transient inward current of peak amplitude dependent on the intensity of the uncaging flash (Fig. 11). The current activated rapidly, and then declined from the peak towards its starting value. The rate of decline, however, was much slower than in the absence of cIMP (Fig. 11, also compare with Fig. 2). The time course of the current decay from its peak was well described by a single exponential with a mean decay time constant of 2.34 ± 1.1 s (range 1.32–3.98, n = 10). The decay time constant in the absence of cIMP was ~0.84 s (see RESULTS). On average, then, the rate of decay of currents activated by uncaging 8Br-cGMP was about threefold slower in the presence of 20 μM cIMP than in its absence (Fig. 11). Mathematical simulations of binding kinetics of the nucleotide to a single site (not shown) indicate that the slowdown in current is consistent with cIMP having reduced the number of available sites for 8Br-cGMP binding by ~70%. Our experimental results are consistent with the proposition that free 8Br-cGMP binds to specific sites in the photoreceptor outer segment and that these sites select cIMP over 8Br-cGMP in a manner similar to that described for rod PDE (Hebert et al., 1998). Data on nucleotide binding are not available for cone outer segments (or cone PDE), but binding is likely quantitatively similar to that in rods since current decay after the uncaging flash was nearly the same in the two photoreceptor types.

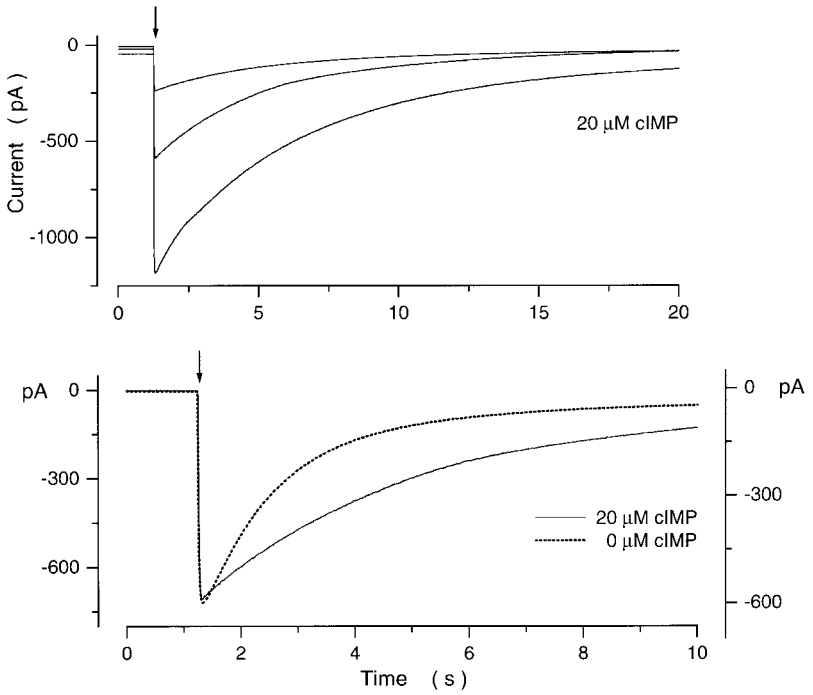

FIGURE 11. Kinetics of membrane currents in tiger salamander dROS activated by uncaging 8Br-cGMP in the presence of 20 μM cIMP added to the cytoplasm. (Top) Currents measured in the same cell at −35 mV holding voltage and generated by uncaging flashes of varying intensity presented at the moment indicated by the vertical arrow. Each flash caused an inward, transient current that did not fully recover its starting value in between flashes. Peak currents (and time after attaining whole-cell mode) were 710 pA (6 min), 172 pA (8 min), and 1,175 pA (10 min). The currents decayed from their peak at a rate well described by a single exponential, yet this rate of decay was slower than that measured under similar conditions but in the absence of cIMP. (Bottom) Flash-activated currents of similar peak amplitude measured in two different dROS. The ordinate scales for the two currents shown are adjusted to match the current's peak amplitude. The continuous trace was measured in the presence of 20 μM cIMP, while the dotted trace was measured in a different dROS in the absence of cIMP.

Submitted: 18 July 2000
Revised: 30 August 2000
Accepted: 2 October 2000

REFERENCES

Barnes, S., and B. Hille. 1989. Ionic channels of the inner segment of tiger salamander cone photoreceptors. *J. Gen. Physiol.* 94:719–743.

Bauer, P.J. 1996. Cyclic GMP-gated channels of bovine rod photoreceptors: affinity, density and stoichiometry of Ca(2+)-calmodulin binding sites. *J. Physiol.* 494:675–685.

Baylor, D.A., and B.J. Nunn. 1986. Electrical properties of the light-sensitive conductance of rods of the salamander Ambystoma tigrinum. *J. Physiol.* 371:115–145.

Bevington, P. 1992. Data reduction and error analysis for the physical sciences. McGraw-Hill Inc., New York. 336 p.

Cameron, D.A., and E.N. Pugh, Jr. 1990. The magnitude, time course and spatial distribution of current induced in salamander rods by cyclic guanine nucleotides. *J. Physiol.* 430:419–439.

Cervetto, L., A. Menini, G. Rispoli, and V. Torre. 1988. The modulation of the ionic selectivity of the light-sensitive current in isolated rods of the tiger salamander. *J. Physiol.* 406:181–198.

Corey, D.P., J.M. Dubinsky, and E.A. Schwartz. 1984. The calcium current in inner segments of rods from the salamander (Ambystoma tigrinum) retina. *J. Physiol.* 354:557–575.

Cote, R.H., and M.A. Brunnock. 1993. Intracellular cGMP concentration in rod photoreceptors is regulated by binding to high and moderate affinity cGMP binding sites. *J. Biol. Chem.* 268: 17190–17198.

Dzeja, C., V. Hagen, U.B. Kaupp, and S. Frings. 1999. Ca^{2+} permeation in cyclic nucleotide-gated channels. *EMBO (Eur. Mol. Biol. Organ.) J.* 18:131–144.

Eismann, E., F. Muller, S.H. Heinemann, and U.B. Kaupp. 1994. A single negative charge within the pore region of a cGMP-gated channel controls rectification, Ca^{2+} blockage, and ionic selectivity. *Proc. Natl. Acad. Sci. USA.* 91:1109–1113.

Forti, S., A. Menini, G. Rispoli, and V. Torre. 1989. Kinetics of phototransduction in retinal rods of the newt Triturus cristatus. *J. Physiol.* 419:265–295.

Frings, S., D.H. Hackos, C. Dzeja, T. Ohyama, V. Hagen, U.B. Kaupp, and J.I. Korenbrot. 2000. Determination of fractional calcium ion current in cyclic nucleotide–gated channels. *Methods Enzymol.* 315:797–817.

Frings, S., R. Seifert, M. Godde, and U.B. Kaupp. 1995. Profoundly different calcium permeation and blockage determine the specific function of distinct cyclic nucleotide–gated channels. *Neuron.* 15:169–179.

Gillespie, P.G., and J.A. Beavo. 1989. Inhibition and stimulation of photoreceptors phosphodiesterase by dipyridamole and M&B 22,948. *Mol. Pharmacol.* 36:773–781.

Gordon, S.E., J. Downing-Park, and A.L. Zimmerman. 1995. Modulation of the cGMP-gated ion channel in frog rods by calmodulin and an endogenous inhibitory factor. *J. Physiol.* 486:533–546.

Gray-Keller, M., W. Denk, B. Shraiman, and P.B. Detwiler. 1999. Longitudinal spread of second messenger signals in isolated rod outer segments of lizards. *J. Physiol.* 519:679–692.

Gray-Keller, M.P., and P.B. Detwiler. 1994. The calcium feedback signal in the phototransduction cascade of vertebrate rods. *Neuron.* 13:849–861.

Hackos, D.H., and J.I. Korenbrot. 1997. Calcium modulation of ligand affinity in the cGMP-gated ion channels of cone photoreceptors. *J. Gen. Physiol.* 110:515–528.

Hackos, D.H., and J.I. Korenbrot. 1999. Divalent cation selectivity is a function of gating in native and recombinant cyclic nucleotide–gated ion channels from retinal photoreceptors. *J. Gen. Physiol.* 113:799–818.

Hagen, V., C. Dzeja, S. Frings, J. Bendig, E. Krause, and U.B. Kaupp. 1996. Caged compounds of hydrolysis-resistant analogues of cAMP and cGMP: synthesis and application to cyclic nucleotide–gated channels. *Biochemistry.* 35:7762–7771.

Hagen, V., C. Dzeja, J. Bendig, I. Baeger, and U.B. Kaupp. 1998. Novel caged compounds of hydrolysis-resistant 8-Br-cAMP and 8-Br-cGMP: photolabile NPE esters. *J. Photochem. Photobiol. B.* 42: 71–78.

Haynes, L.W. 1995. Permeation of internal and external monovalent cations through the catfish cone photoreceptor cGMP-gated channel. *J. Gen. Physiol.* 106:485–505.

Haynes, L.W., and K.-W. Yau. 1990. Single channel measurement from the cGMP-activated conductance of catfish retinal cones. *J. Physiol.* 429:451–481.

He, Y., M. Ruiz, and J.W. Karpen. 2000. Constraining the subunit order of rod cyclic nucleotide-gated channels reveals a diagonal arrangement of like subunits. *Proc. Natl. Acad. Sci. USA.* 97:895–900.

Hebert, M.C., F. Schwede, B. Jastorff, and R.H. Cote. 1998. Structural features of the noncatalytic cGMP binding sites of frog photoreceptor phosphodiesterase using cGMP analogs. *J. Biol. Chem* 273:5557–5565.

Hestrin, S., and J.I. Korenbrot. 1987. Effects of cyclic GMP on the kinetics of the photocurrent in rods and in detached rod outer segments. *J. Gen. Physiol.* 90:527–551.

Hestrin, S., and J.I. Korenbrot. 1990. Activation kinetics of retinal cones and rods: response to intense flashes of light. *J. Neurosci.* 10:1967–1973.

Hodgkin, A.L., P.A. McNaughton, and B.J. Nunn. 1985. The ionic selectivity and calcium dependence of the light-sensitive pathway in toad rods. *J. Physiol.* 358:447–468.

Hsu, Y.T., and R.S. Molday. 1993. Modulation of the cGMP-gated channel of rod photoreceptor cells by calmodulin. *Nature.* 361: 76–79.

Kao, J.P., and R.Y. Tsien. 1988. Ca^{2+} binding kinetics of fura-2 and azo-1 from temperature-jump relaxation measurements. *Biophys. J.* 53:635–639.

Karpen, J.W., A.L. Zimmerman, L. Stryer, and D.A. Baylor. 1988. Gating kinetics of the cyclic-GMP-activated channel of retinal rods: flash photolysis and voltage-jump studies. *Proc. Natl. Acad. Sci. USA.* 85:1287–1291.

Korenbrot, J.I. 1995. Ca^{2+} flux in retinal rod and cone outer segments: differences in Ca^{2+} selectivity of the cGMP-gated ion channels and Ca^{2+} clearance rates. *Cell Calc.* 18:285–300.

Koutalos, Y., R.L. Brown, J.W. Karpen, and K.W. Yau. 1995. Diffusion coefficient of the cyclic GMP analog 8-(fluoresceinyl) thioguanosine 3′,5′ cyclic monophosphate in the salamander rod outer segment. *Biophys. J.* 69:2163–2167.

Lagnado, L., L. Cervetto, and P.A. McNaughton. 1992. Calcium homeostasis in the outer segments of retinal rods from the tiger salamander. *J. Physiol.* 455:111–142.

Maricq, A.V., and J.I. Korenbrot. 1988. Calcium and calcium-dependent chloride currents generate action potentials in solitary cone photoreceptors. *Neuron.* 1:503–515.

Maricq, A.V., and J.I. Korenbrot. 1990. Potassium currents in the inner segment of single retinal cone photoreceptors. *J. Neurophysiol.* 64:1929–1940.

Miller, D.L., and J.I. Korenbrot. 1987. Kinetics of light-dependent Ca fluxes across the plasma membrane of rod outer segments: a dynamic model of the regulation of the cytoplasmic Ca concentration. *J. Gen. Physiol.* 90:397–425.

Miller, J.L., and J.I. Korenbrot. 1993. Phototransduction and adaptation in rods, single cones, and twin cones of the striped bass retina: a comparative study. *Vis. Neurosci.* 10:653–667.

Miller, J.L., and J.I. Korenbrot. 1994. Differences in calcium homeostasis between retinal rod and cone photoreceptors revealed

by the effects of voltage on the cGMP-gated conductance in intact cells. *J. Gen. Physiol.* 104:909–940.

Nakatani, K., and K.W. Yau. 1988. Calcium and magnesium fluxes across the plasma membrane of the toad rod outer segment. *J. Physiol.* 395:695–729.

Nakatani, K., and K.W. Yau. 1989. Sodium-dependent calcium extrusion and sensitivity regulation in retinal cones of the salamander. *J. Physiol.* 409:525–548.

Neher, E. 1995. The use of fura-2 for estimating Ca buffers and Ca fluxes. *Neuropharmacology.* 34:1423–1442.

Nikonov, S., N. Engheta, and E.N. Pugh, Jr. 1998. Kinetics of recovery of the dark-adapted salamander rod photoresponse. *J. Gen. Physiol.* 111:7–37.

Olson, A., and E.N. Pugh Jr. 1993. Diffusion coefficient of cyclic GMP in salamander rod outer segments estimated with two fluorescent probes. *Biophys. J.* 65:1335–1352.

Perry, R.J., and P.A. McNaughton. 1991. Response properties of cones of the retina of the tiger salamander. *J. Physiol.* 433:561–587.

Picones, A., and J.I. Korenbrot. 1992. Permeation and interaction of monovalent cations with the cGMP-gated channel of cone photoreceptors. *J. Gen. Physiol.* 100:647–673.

Picones, A., and J.I. Korenbrot. 1995. Permeability and interaction of Ca^{2+} with cGMP-gated ion channels differ in retinal rod and cone photoreceptors. *Biophys. J.* 69:120–127.

Rebrik, T.I., and J.I. Korenbrot. 1998. In intact cone photoreceptors, a Ca^{2+}-dependent, diffusible factor modulates the cGMP-gated ion channels differently than in rods. *J. Gen. Physiol.* 112: 537–548.

Rispoli, G., W.A. Sather, and P.B. Detwiler. 1993. Visual transduction in dialysed detached rod outer segments from lizard retina. *J. Physiol.* 465:513–537.

Root, M.J., and R. Mackinnon. 1993. Identification of an external divalent cation-binding site in the pore of a cGMP-activated channel. *Neuron.* 11:459–466.

Sagoo, M.S., and L. Lagnado. 1996. The action of cytoplasmic calcium on the cGMP-activated channel in salamander rod photoreceptors. *J. Physiol.* 497:309–319.

Seifert, R., E. Eismann, J. Ludwig, A. Baumann, and U.B. Kaupp. 1999. Molecular determinants of a Ca^{2+}-binding site in the pore of cyclic nucleotide-gated channels: S5/S6 segments control affinity of intrapore glutamates. *EMBO (Eur. Mol. Biol. Organ.) J.* 18: 119–130.

Shammat, I.M., and S.E. Gordon. 1999. Stoichiometry and arrangement of subunits in rod cyclic nucleotide-gated channels. *Neuron.* 23:809–819.

Sneyd, J., and D. Tranchina. 1989. Phototransduction in cones: an inverse problem in enzyme kinetics. *Bull. Math. Biol.* 51:749–784.

Tanaka, J.C., J.F. Eccleston, and R.E. Furman. 1989. Photoreceptor channel activation by nucleotide derivatives. *Biochemistry.* 28: 2776–2784.

Torre, V., S. Forti, A. Menini, and M. Campani. 1990. Model of phototransduction in retinal rods. *Cold Spring Harbor Symp.Quant. Biol.* 55:563–573.

Wells, G.B., and J.C. Tanaka. 1997. Ion selectivity predictions from a two-site permeation model for the cyclic nucleotide–gated channel of retinal rod cells. *Biophys. J.* 72:127–140.

Yau, K.W., and K. Nakatani. 1985. Light-induced reduction of cytoplasmic free calcium in retinal rod outer segment. *Nature.* 313: 579–582.

Younger, J.P., S.T. McCarthy, and W.G. Owen. 1996. Light-dependent control of calcium in intact rods of the bullfrog *Rana catesbeiana. J. Neurophysiol.* 75:354–366.

Zimmerman, A.L., G. Yamanaka, F. Eckstein, D.A. Baylor, and L. Stryer. 1985. Interaction of hydrolysis-resistant analogs of cyclic GMP with the phosphodiesterase and light-sensitive channel of retinal rod outer segments. *Proc. Natl. Acad. Sci. USA.* 82:8813–8817.

Zimmerman, A.L., and D.A. Baylor. 1992. Cation interactions within the cyclic GMP-activated channel of retinal rods from the tiger salamander. *J. Physiol.* 449:759–783.